Title
THE EFFECTS OF SO2 AND SO3 ON THE Na2SO4-INDUCED CORROSION OF NICKEL

Authors
Misra, A.K.
Whittle, D.P.

Publication Date
1982-05-01

Lawrence Berkeley Laboratory
UNIVERSITY OF CALIFORNIA

Materials & Molecular Research Division

Submitted to Oxidation of Metals

THE EFFECTS OF SO_2 AND SO_3 ON THE Na_2SO_4-INDUCED CORROSION OF NICKEL

A.K. Misra and D.P. Whittle

May 1982

Prepared for the U.S. Department of Energy under Contract DE-AC03-76SF00098

DISCLAIMER

THE EFFECTS OF SO_2 AND SO_3 ON THE Na_2SO_4-INDUCED CORROSION OF NICKEL

A. K. Misra and D. P. Whittle

Lawrence Berkeley Laboratory
and Department of Materials Science and Mineral Engineering
University of California
Berkeley, California 94720

ABSTRACT

The effects of SO_2 and SO_3 in the environment on the hot corrosion behavior of Ni in the temperature range 750 to 950°C has been studied. Below the melting point of Na_2SO_4 (880°C) rapid corrosion takes place by formation of a Na_2SO_4-$NiSO_4$ melt which can penetrate the porous oxide scale and give rise to sulfide formation. The distribution of the sulfides depends on the SO_3 + SO_2 level in the ambient gas. Continued corrosion occurs by a sulfidation-oxidation mechanism. At temperatures above the melting point of Na_2SO_4, accelerated degradation proceeds via dissolution on the surface scale, followed by re-precipitation of the oxide in a non-protective form.

This work was supported by the Director, Office of Energy Research, Office of Basic Energy Sciences, Materials Sciences Division of the U. S. Department of Energy under Contract Number DE-AC03-76SF00098.

1. INTRODUCTION

Hot corrosion in gas turbines, operating in marine environments is attributed to the deposition of Na_2SO_4 on the blade and vane surfaces. The temperature of blade surface depends on the nature of operation of the gas turbine and accordingly if the temperature is above the melting point of Na_2SO_4 (884°C), as is usual in aero-engine operation, the deposit is molten. Lower power gas turbines (e.g. marine shipboard propulsion, some industrial units), more commonly operate with blade temperatures, in the range 650-850°C which is below the melting point of Na_2SO_4. In addition, the SO_3 concentration in the turbine atmosphere is of the order of 10^{-3}-10^{-5} atm. This SO_3 is particularly important for hot corrosion below the melting point of Na_2SO_4. Under these conditions, corrosion is initiated by the formation of low melting mixed sulfates (1, 2); however, the factors affecting the propagation of corrosion are not well characterized. Luthra and Shores (4) have studied the effect of SO_3 on the Na_2SO_4 induced corrosion behavior of cobalt base alloys at temperatures below the melting point of Na_2SO_4. They describe a mechanism, in which cobalt oxide dissolves as Co^{++} at the salt-oxide interface, and is re-precipitated as Co_3O_4 at the salt-gas interface. On the other hand, Jones et al. (4, 5) attributed the rapid corrosion to the decomposition of the mixed sulfate melt by coming in contact with the alloy, followed by sulfide formation inside the alloy.

At temperatures, above the melting point of Na_2SO_4, the presence of SO_3 in the atmosphere can also lead to dissolution of oxides as sulfates. However, this has not been studied in detail. Goebel and Pettit (6) described the dissolution process a fluxing mechanism in which the protective oxides are dissolved in the Na_2SO_4 melt via either an acidic or basic

fluxing mechanism, depending on the Na_2O activity in the melt. In the acidic fluxing mechanism, described for the rapid corrosion of Ni base alloys containing W, Mo, V, the dissolution of NiO and Al_2O_3 as sulfates was possible due to the low Na_2O activity in the melt. However, in their experiments, the atmosphere above the melt did not contain SO_3, and the low Na_2O activity was generated at the oxide-salt interface by the reaction of acidic oxides like V_2O_5, MoO_3 or WO_3 with the oxide ions in the melt. The dissolved sulfates were converted to their respective oxides at the salt-gas interface where the Na_2O activity was higher. This continuous dissolution and reprecipitation process was responsible for the catastrophic corrosion of nickel base alloys containing W, Mo or V. When the atmosphere above the melt contains SO_2, the Na_2O activity at the salt-gas interface will be higher than, or equal to that at the oxide-salt interface, and a different corrosion mechanism operative.

Kofstad et al. (7) studied the effect of 4% SO_2 in the atmosphere on the Na_2SO_4-induced corrosion behavior of nickel at 900°C. The solubility of SO_2 in the Na_2SO_4 melt is negligible (8), whereas SO_3 has a high solubility as a result of $Na_2S_2O_7$ formation (9). Kofstad's experimental system did not contain a catalyst, and it is unlikely that the gas mixture would contain other than trace amounts of SO_3. He attributed the rapid corrosion to the development of a porous scale and the formation of sulfides at the scale-metal interface. Cutler and Grant (10) also attributed the rapid corrosion of stainless steel in Na_2SO_4-Li_2SO_4 melts in atmospheres containing SO_3 to the formation of sulfide within the alloy.

The present investigation is aimed at obtaining a better understanding of the effect of SO_2 + SO_3 on the Na_2SO_4 induced corrosion behavior of nickel. The temperature range of interest is 750-923°C, which includes

temperatures both above and below the melting point of Na_2SO_4. As indicated earlier, formation of the mixed sulfate melt is the first step in the corrosion process, and the sulfation process itself must be understood. Thus, in addition to the actual corrosion behavior, the kinetics of sulfation of NiO in the presence of Na_2SO_4 has also been studied.

2. EXPERIMENTAL PROCEDURE

The experimental apparatus used is similar to that described in an earlier publication (11). For corrosion experiments, instead of a platinum crucible, the metal sample was hung from a platinum wire. Briefly, the experimental apparatus consisted of a catalyst furnace and a reaction furnace. In order to attain the equilibrium between SO_2, SO_3 and O_2, the gas mixture was passed through a catalyst furnace before entering the reaction furnace.

The samples used in the present study are commercially pure nickel of 99.5% purity. The specimens, rectangular coupons approximately of size 10x10x1 mm. were ground through 600 grit SiC papers and after grinding, cleaned with alcohol and acetone before the start of the experiments. The samples were coated with the Na_2SO_4 deposit by spraying an aqueous Na_2SO_4 solution over the sample, heated to 300°C on a hot plate. Visual examination of the deposit showed it to be uniform over all the sample surface. The Na_2SO_4 coated samples were exposed to an atmosphere consisting of air plus specified amount of SO_2-SO_3 at different temperatures. The kinetics of corrosion were measured by periodically taking out the sample from the furnace and monitoring the weight gain. Corroded samples were analyzed by metallography, x-ray diffraction, scanning electron microscopy and electron probe micro-analysis.

The kinetics of sulfation of NiO in the presence of Na_2SO_4 was measured by exposing a platinum crucible containing a mixture of Na_2SO_4+NiO, to an atmosphere containing specified levels of Air + SO_2-SO_3 and monitoring the weight gain with time. Reagent grade Na_2SO_4 and NiO powders were used and the size of the individual Na_2SO_4 or NiO particles was very small, approximately 5-10μm. The total weight of Na_2SO_4+NiO mixture was approximately 0.45 gm and this occupied only 1/2 mm depth inside the platinum crucible.

3. RESULTS

a. Kinetics of Sulfation of NiO in the Presence of Na_2SO_4

Figure 1 shows the sulfation kinetics at three different P_{SO_3} levels in the atmosphere. The time required for liquid formation at 750°C decreases with an increase in P_{SO_3} level in the atmosphere. For example, when the atmosphere contains 10% SO_2 (P_{SO_3} = 3.8×10^{-2} atm.), the liquid could be formed in 15-20 mintues (curve A), whereas approximately 2 hrs. were required for the liquid to be formed when the atmosphere contained 1.1% SO_2 (P_{SO_3} = 7.28×10^{-3} atm.)(curve B). At even lower levels of SO_2 in the atmosphere (0.104%), it took even longer (15-16h) for the liquid to be formed.

Linear kinetics were observed until liquid formed. The rate-controlling step was not identified. Once liquid formed, the raction rate decreased with time, suggesting a diffusion-controlled reaction mechanism. Sulfation experiments were also carried out at 923°C. At this temperature, the reaction took place in the presence of a melt from the very beginning. The weight gain curve is also plotted in Figure 9 (curve D).

On account of the very small size of the individual NiO particles,

the total initial surface area of the particles is large. Thus, any increase in the particle surface area due to sulfation will be negligible. In addition, any resistance to diffusion in the pores between the particles can be neglected. Thus, for the analysis of the kinetic results, a flat plate approximation can be made. Based on this approximation, Figure 2 shows that a plot of (weight gain)^2 versus time is linear, both at 750°C and 923°C, confirming that diffusion through the melt is the rate controlling step for sulfation, once liquid has formed. At 750°C, the point corresponding to liquid formation in Figure 1 was taken as the initial datum point.

In the present experiments, the Na_2SO_4 + NiO mixture is highly porous, and during the solid state sulfation process, the reacting gases can freely pass through the space between the particles, reach the particle surface, and form sulfate. After the formation of the liquid, or when the liquid is present from the beginning (i.e., at temperatures > the m.p. of Na_2SO_4), every NiO particle becomes covered with a thin layer of liquid. The liquid also covers the top surface of the mixture. Thus, the reacting gas, SO_3, has to diffuse through the melt in order to reach the NiO surface, and a significant SO_3 gradient must exist through the melt, even though the maximum thickness of liquid is only 0.5 mm, the depth occupied by the Na_2SO_4 + NiO mixture in the platinum crucible. This has an important bearing on the corrosion process, as discussed later.

b. Corrosion Kinetics at 750°C

Figure 3a shows the weight gain curves at 750°C for nickel, coated with 1.5 mg/cm^2 Na_2SO_4 and exposed to three different SO_3 levels in the atmosphere. The rate of corrosion increases with increase in P_{SO_3}. At

the lowest SO_2 level, 0.104% (P_{SO_3} = 6.8×10^{-4} atm), the initial rate of corrosion is very slow and is related to the long time required for liquid formation: sulfation kinetic measurements showed this to take some 15-16 hours. However, at longer times (Figure 3b), the weight gain is comparable to that in atmospheres containing higher levels of SO_2 of Ni in Air or O_2 at 750°C. For comparison, using the parabolic rate constant for nickel oxidation in air or O_2 at 750°C (12), the weight gain would be approximately 0.1 mg/cm^2 after 120 min. exposure; measurements in this work in air containing 1.1% SO_2 (P_{SO_3} = 7.28×10^{-3} atm), but no sulfate deposit gave 0.6 mg/cm^2 after 60 min. Clearly, there is a tremendous increase in the rate of oxidation in the presence of a Na_2SO_4 deposit, particularly in atmospheres containing SO_2, SO_3.

On account of the non-uniform nature of the corrosion, as described later, it is inappropriate to attempt to identify a rate-controlling step, solely on the basis of kinetic data.

c. Corrosion Kinetics at 923°C

Figure 4 shows data similar to Figure 3, but at 923°C. The weight gain curves show an initial rapid increase in the corrosion rate, followed by a decrease. It is surprising to note that the initial rate is higher in the 0.104% SO_2 atmosphere than in that containing 1.1% SO_2. Figure 4 also shows the weight gains obtained in the presence of a molten Na_2SO_4 deposit only (no SO_2 + SO_3): the presence of even small amounts of SO_2 increase the corrosion rate 8-10 times.

d. Scale Morphology at 750°C

Figure 5 show a cross section of nickel, coated with 1.5 mg/cm^2 Na_2SO_4 and oxidized for 30 minutes in an atmosphere consisting of air + 1.1% SO_2 (P_{SO_3} = 7.28×10^{-3} atm). A NiO layer is present above the

metal surface. The Na_2SO_4-$NiSO_4$ melt has formed and penetrated the oxide to reach the oxide-metal interface. Melt penetration through the oxide appears to be primarily along the oxide grain boundaries. Void formation at the oxide-metal interface, and the metal grain boundaries adjacent to this interface is also evident. The melt has penetrated the oxide grain boundaries filling the voids at the oxide-metal interface, and in this process, some oxide grains are completely detached from the metal and lifted off. This penetration of melt through the oxide grain boundaries occurs irrespective of the SO_3 level in the atmosphere.

After the melt penetrates the oxide and fills the voids at the scale-metal interface, it is in direct contact with the metal and the subsequent scale morphology, depends on the SO_3 level in the atmosphere. Figure 6 shows a cross-section after 2 hours oxidation in air containing 1.1% SO_2 ($P_{SO_3} = 7.28 \times 10^{-3}$ atm). A nodular type of scale is formed, the outermost, thin NiO layer, being highly porous. This outermost NiO layer is formed before the melt formation and is detached at several locations, because of melt penetration through it. The layered type of scale below, is formed after the melt penetrates the oxide and consists of (1) a thick intermixed oxide + sulfide (NiO + Ni_3S_2) duplex scale, (2) a layer of NiO just below this, and (3) a layer of sulfide (Ni_3S_2) at the oxide-metal interface. The NiO, just below the intermixed oxide + sulfide scale, appears to be formed preferentially along the grain boundaries. This leaves some unoxidized grains in the NiO scale, whereas oxides continue to form along grain boundaries deeper into the metal. The sulfides at the scale-metal interface are also formed along grain boundaries. Sulfides are also observed at the interface between the

unoxidized grain inside the oxide scale and the oxide scale.

When the atmosphere contains 0.104% SO_2 (P_{SO_3} = 6.81×10^{-4} atm), the inner part of the scale is similar to that described above. Oxides are formed first along grain boundaries, whilst the sulfides are formed at the grain boundary oxide-grain interface (Fig. 7). With progress of time, the complete grain,along with the sulfides are oxidized, forming a continuous NiO layer, while sulfides are again re-formed at the oxide-metal interface, preferentially along the grain boundaries (Fig. 8). Figures 7 and 8 also show an outer porous NiO layer, which is formed before the formation of the melt. A significant feature of the scale formed under these conditions is a Ni_2O_3 layer just below the outermost porous NiO layer. This phase was confirmed by x-ray diffraction. (See Table 1.) It is formed after the melt had penetrated the outermost oxide layer and reached the metal surface. Ni_2O_3 is not stable at the partial pressures of oxygen, used in the present experiments (0.21 atm). Since Ni_2O_3 is not normally formed by the high temperature oxidation process under these experimental conditions, it might have formed by decomposition of the $NiSO_4$ component of the Na_2SO_4-$NiSO_4$ melt. To confirm this, further experiments were carried out to study the decomposition behavior of the melt.

e. Nature of the Decomposition of the Na_2SO_4-$NiSO_4$ Melt

A mixture of Na_2SO_4-$NiSO_4$ was placed in a platinum crucible and heated in air. At 750°C the melt, upon decomposition, produced a thin, dark, grey layer at the surface; Fgiure 9, shows the surface topography of the solidified melt. X-ray diffraction identified this dark, grey layer as Ni_2O_3. (The x-ray diffraction data for Ni_2O_3 are given in Table 1.) Similar decomposition studies at 923°C showed the decomposi-

tion product to be Ni_2O_3, only during the first few minutes of decomposition. When the decomposition experiments were carried out for longer times, the dark greyish Ni_2O_3 layer was gradually coverted to a greenish NiO layer. At 750°C, the Ni_2O_3-NiO transformation is slow, and even after long decomposition periods, the product is Ni_2O_3. Thus, it is clear the Na_2SO_4-$NiSO_4$ melt decomposes to metastable Ni_2O_3 which is slowly converted to NiO. The transformation is particularly sluggish at the lower temperatures.

f. Scale Morphology at 923°C

At 923°C, Na_2SO_4 is molten, and the corrosion of nickel takes place beneath a melt from the very beginning. Figure 10 shows the cross-section of nickel, coated with 0.55 mg/cm^2 Na_2SO_4 and exposed to an atmosphere containing 0.104% SO_2 in air (P_{SO_3} = 1.2x10^{-4} atm.) for 45 minutes. The outer porous NiO layer appears to have been formed by a precipitation process. It is similar to that obtained by Goebel and Pettit (13) in their experiments on the corrosion of nickel in the presence of Na_2SO_4 only at 1000°C. In addition, NiO is also formed along grain boundaries inside the metal. It appears that the oxides are formed at the grain boundaries first, and grow laterally. The melt also penetrates the oxide along grain boundaries and forms a layer at the oxide-metal interface. Figure 10b shows the scale-metal interface at a higher magnification and it can be seen that a part of the melt has decomposed. This type of morphology suggests that once the melt penetrates the scale and reaches the metal surface, its decomposition supplies oxidants for further oxidation of the metal. When the amount (thickness) of the Na_2SO_4 deposit is increased, similar scale morphologies are observed. However, the thickness of the outer precipitated NiO layer increases, whilst the inner part of the scale consists of NiO, the melt and the

decomposition products of the melt (Figure 11) is unchanged. At the oxide-metal interface, oxides are again preferentially formed along the grain boundaries.

In contrast, for atmospheres containing 1% SO_2 in Air, there is a strong dependence on the amount of Na_2SO_4 deposit. Figure 12 shows the cross-section of nickel, coated with 0.1 mg/cm^2 Na_2SO_4 and oxidized in an atmosphere containing 1.1% SO_2 in air for 1 hr. As in Figure 10, there is an outer, porous oxide layer, formed by precipitation. However, the oxide is not NiO, but a mixture of NiO (light) and Ni_2O_3 (dark). Figure 12b shows the details: NiO is concentrated towards the outer part, and Ni_2O_3 layer at the inner part. Earlier while studying the decomposition of the Na_2SO_4-$NiSO_4$ melt, it was indicated that Ni_2O_3 is a metastable phase, and gradually transforms to NiO. Thus, the outer porous layer must have been Ni_2O_3 originally, with the Ni_2O_3-NiO transformation starting at the oxide-gas interface. When the initial amount of Na_2SO_4 deposit is increased to 1 mg/cm^2, the scale has an outer porous NiO layer (Figure 13), similar to that of Figure 10. Thus, increase in the amount of the Na_2SO_4 deposit modifies the precipitation process, and changes the nature of the outer porous oxide layer. An additional feature of the scale in Figure 13 is the formation of liquid sulfides at the oxide-metal interface.

When the ambient atmosphere contains 10% SO_2, the extent of corrosion is again dependent on the amount of Na_2SO_4 deposit on the sample, increasing with increasing amount of deposit, although, the morphology does not change significantly. Figures 14-16 show the evolution of the scale with time. During the first few minutes of oxidation beneath the melt, oxides are formed preferentially along the alloy grain

boundaries (Figure 14). Examination of the outer scale at a higher magnification shows a thin layer of NiO + Ni_2O_3 precipitates at the melt-gas interface (Figure 14b). After longer times, the melt penetrates the oxides, along grain boundaries and comes in contact with the metal (Figure 15). This leaves some unoxidized grains towards the oxide-gas interface. Further oxidation of nickel takes place beneath the melt, the oxidants being supplied by the decomposition of the melt; a layered type of scale, consisting of sulfides beneath the oxide, is developed. After even longer times, the unoxidized grains are oxidized, and most of the melt disappears, presumably by decomposition (Figure 16). The scale shows a thick NiO scale, with only small amounts of melt dispersed in it.

4. DISCUSSION

a. Corrosion Behavior at Temperatures Below the Melting Point of Na_2SO_4

1. Degradation Process Before the Melt Formation:

Nickel, upon oxidation forms NiO. In the presence of a Na_2SO_4 deposit and a small amount of $SO_3(g)$ in the atmosphere, NiO dissolves in Na_2SO_4 to form a Na_2SO_4-$NiSO_4$ solid solution until the total $NiSO_4$ content corresponds to the liquidus composition in the Na_2SO_4 rich portion of the Na_2SO_4-$NiSO_4$ phase diagram. Before melt formation, the rate of corrosion of nickel is dependent on the various factors affecting the rate of formation of NiO and its rate of sulfation. However, two limiting cases can be described:

Case 1: Rate of oxidation of Ni >> rate of sulfation of NiO. In this case, the rate of corrosion will be independent of the sulfation-process, and is similar to that for pure oxidation.

Case 2: Rate of sulfation of NiO >> rate of oxidation of Ni. In this case, the rate of corrosion will be the same as that of the rate of sulfation of the oxide. The

thickness of the oxide layer between the nickel and the sulfate layer will be very thin.

In the present studies, the weight gain for the oxidation of nickel, in the presence of a Na_2SO_4 deposit and $SO_3(g)$ in the atmosphere, is much higher than that of oxidation in the absence of a Na_2SO_4 deposit. For instance, the weight gain for a sample coated with 1.5 mg/cm^2 Na_2SO_4 and in an atmosphere containing 1.1% SO_2 in air after 30 minutes, is about 2 mg/cm^2 compared to 0.6 mg/cm^2 after 60 minutes in the same gas mixture, but without the deposit. This indicates that before the melt formation, the corrosion rate is controlled by the rate of NiO sulfation.

A compact NiO layer on nickel is known to grow by the outward migration of cations and electrons (14). In addition, voids can be introduced at the scale-metal interface and within the metal, and if consumption of the metal is not readily accommodated by plastic deformation of the scale, the scale begins to lose contact with the metal. These mechanisms of void formation and loss of contact between the scale and metal have been described by numerous workers (15-17).

In the presence of a Na_2SO_4 deposit and SO_3 in the atmosphere, NiO dissolves as $NiSO_4$, the dissolution process leading to an increased consumption of Ni. Thus, the potential number of vacancies entering the metal lattice is higher than that for simple oxidation, with an increasing tendency to create voids both at metal grain boundaries and at the scale-metal interface. Scale-metal detachment, due to the inability of the scale to deform plastically, is commonly observed during oxidation of nickel at temperatures as high as 1100-1200°C (18), and plastic deformation

of the NiO scale will be more difficult at 750°C. Thus, this combination of factors causes the scale to lose contact with the metal at a very early stage of the oxidation process.

Once the scale loses contact with the metal, further oxidation can continue by a dissociation mechanism, described in detail by Mrowec (19). In this, NiO above the voids dissociation to supply O_2 for the oxidation of nickel beneath. Continuation of this process eventually leads to a porous scale.

The mechanism of sulfation of oxides to form a solid sulfate is not yet clear. Hocking and Alcock (20) studied the solid state sulfation of CoO to form $CoSO_4$ under non Co_3O_4 forming conditions. There was no Na_2SO_4 deposit in their experiments. The sulfate ($CoSO_4$) grew outwards from the oxide surface, and they suggested that M^{++} ions and electrons leave the oxide and diffuse through the MSO_4 product layer to the sulfate-gas interface. The gas is a mixture of SO_3 and O_2. The oxygen is reduced to $O^{=}$, which combines with SO_3 to form $SO_4^{=}$. M^{++} combines with $SO_4^{=}$ to give MSO_4 at the sulfate-gas interface. Since the M^{++} ions leave the oxide lattice and diffuse through the sulfate to the sulfate-gas interface, vacant cation sites are created in the oxide lattice, which can condense to form voids.

Very few studies have been made on the sulfation of NiO. From the limited studies of Hocking and Alcock (21), it is evident that NiO, prepared by the oxidation of Ni, sulfated very slowly. However, there was rapid sulfation of NiO, prepared by decomposition of $NiSO_4$. This was attributed to the presence of sulfur in NiO, and marker studies indicated inward growth of $NiSO_4$, which suggested that SO_3

diffuses through the sulfate layer and reacts with the oxide at the oxide-sulfate interface. Nevertheless, the sulfation mechanism for NiO, grown by oxidizing nickel, should be similar to that described by Hocking and Alcock (20) for CoO under non Co_3O_4 forming conditions (the CoO blcoks were prepared by oxidizing Co).

Assuming that this sulfation mechanism (20) is valid, than at some stage, the sulfate should lose contact with the oxide in a manner similar to that for the oxidation of metals. In the presence of Na_2SO_4, the rate of sulfation is higher than that without the Na_2SO_4 (22) and it is anticipated that the loss of contact will occur at an early stage of the sulfation process. Further sulfation occurs by some other mechanism, possibly the transport of SO_3 through the sulfate layer or a dissociation mechanism will operate. However, one of the important consequences of the mechanism, described by Hocking and Alcock (20), is the introduction of voids in the oxide, and it will be seen later that the voids help in the penetration of the melt through the oxide.

In the present investigation, the melt, after it is formed, penetrates, the oxide layer and reaches the metal surface. This can be explained, on the basis of either of the following mechanisms:

i. Melt Penetration Through Oxide Grain Boundaries:

Assume that a porous NiO scale is not developed during the oxidation or sulfation process. Firstly, a melt corresponding to the liquidus composition in the Na_2SO_4 rich portion of the Na_2SO_4-$NiSO_4$ phase diagram will be formed. If the liquidus composition in the Na_2SO_4 rich portion of the Na_2SO_4-$NiSO_4$ phase diagram is lower than the equilibrium $NiSO_4$ content of

the liquid corresponding to the P_{SO_3} in the atmosphere, this liquid will dissolve more NiO. It was mentioned earlier, that after the formation of the liquid, the rate of sulfation is slow and is controlled by the diffusion of reactants through the melt. Thus, after the melt formation, the rate of sulfation may or may not be higher than the rate of oxidation of Ni to form NiO. If the rate of oxidation of nickel to form NiO is higher than the rate of sulfation, then the thickness of NiO layer will increase. The NiO at the grain boundaries is preferentially dissolved in the melt. This is similar to the leaching of metal grain boundaries by liquid sulfides that is observed during sulfidation of Fe at high temperatures (23). Thus, the melt slowly penetrates the oxide grain boundaries by dissolving the oxide there, and a morphology similar to Figure 5 is developed.

ii. Penetration of Melt Through the Pores in Oxide:

Assume that a porous NiO scale has been developed either as a result of the oxidation process or the sulfation process or a combination of both. If the former is the case, then, a thin compact layer of NiO might be present above the porous oxide layer. However, the thin compact layer of oxide can be dissolved during the sulfation process. Now, the liquid fills the pores next to the melt, and oxides next to the pores are dissolved in the melt. Thus, by successively filling the pores and dissolving the oxides, the melt can reach the metal surface. Some of the pores might also be interconnected, and the melt can directly pass through these pores to come in contact with

the metal.

2. Interaction of the Metal with the Melt and Transport of Gases Through Melt:

After the melt penetrates the oxide layer and comes in contact with the metal surface, further degradation of the metal will be dependent on the interaction of the melt with the metal. This is best understood using the Na-Ni-S-O stability diagram (Figure 17) which shows the stability of various phases as a function of P_{O_2} and P_{SO_3}.

From this diagram, it is evident that Ni cannot coexist along with the Na_2SO_4-$NiSO_4$ melt. Thus, upon coming in contact with the Na_2SO_4-$NiSO_4$ melt, it must convert either to NiO or Ni_3S_2 or a mixture of the two. The oxidants required for the oxidation process are supplied to the metal surface by transport through the Na_2SO_4-$NiSO_4$ melt, and is dependent on their solubility.

The solubilities of O_2 and SO_2 in the melt are very low (8), and cannot account for the rapid weight gain, observed in the corrosion experiments. On the other hand, SO_3 has a higher solubility because of the $SO_4^{=}$ - $S_2O_7^{=}$ equilibrium, thus, SO_3 is the major oxidizing species once the melt comes in direct contact with the metal.

3. Decomposition of the Melt:

As indicated in the previous section, the oxidation and sulfidation of Ni beneath the Na_2SO_4-$NiSO_4$ melt involves transport of SO_3 through the melt. If the rate of SO_3 consumption at the metal/scale interface is greater than the maximum rate of transport through the melt, then there will be an SO_3 gradient through the

melt, as seemed to be also the case in the studies of NiO sulfation. If the P_{SO_3} at the melt/metal interface is lower than that at the melt/gas interface, then it is possible that decomposition of the melt in contact with the metal takes place, as observed for low SO_3 concentrations in the ambient atmosphere. Indeed, at 750°C, the minimum P_{SO_3} required for liquid formation in the Na_2SO_4-$NiSO_4$ system is 5.62×10^{-4} atm. (11), and in air + 0.104% SO_2, the equilibrium P_{SO_3} is only just greater than this: 6.86×10^{-4} atm. As a consequence, even a slight decrease in P_{SO_3} at the melt/metal interface would cause the melt to decompose there, as observed. In contrast, in air + 1.1% SO_2, the equilibrium P_{SO_3} is 7.26×10^{-3} atm., and thus a substantial gradient in P_{SO_3} would be necessary before salt decomposition at the melt/metal interface would be expected.

4. Formation of Sulfides and Development of Scale Morphology Beneath the Melt:

In the presence of Na_2SO_4, the scale dissolves in Na_2SO_4, and the resulting Na_2SO_4-$NiSO_4$ melt, by penetrating through the oxide, reaches the metal surface. It was indicated earlier that only SO_3 can be transported across the melt, thus, SO_3 is the principal oxidizing species. The situation here is analogous to the oxidation behavior in atmospheres containing SO_2 and SO_3, which has been studied by several workers in the recent past (24-28). In the presence of SO_3, the overall degradation reaction can be written as

$$9Ni + 2SO_3 = Ni_3S_2 + 6NiO \qquad [1]$$

The scale morphology, that is obtained after oxidation in an atmosphere containing SO_2 or SO_3, consists of an outer mixed oxide + sulfide layer and a sulfide layer at the scale-metal interface

(24-28). The exact mode of development of this type of scale morphology is not clear and still an active area of research. Luthra and Worrell (27), in their studies on the oxidation of nickel in argon + SO_2 atmospheres suggest that initially a porous NiO layer is formed and after the initial period, sulfides are formed both at the scale-metal interface and inside the porous oxide scale. Singh and Birks (24) have studied the oxidation of cobalt in argon + SO_2 atmospheres and their results show that initially a scale consisting of sulfides beneath the oxide is formed. However, eventually sulfides form within the oxide scale, resulting in a mixed oxide + sulfide outer scale.

Thus, after the melt penetrates the oxide and reaches the metal surface, during the initial period of oxidation, a layered scale consisting of sulfides beneath an outer porous NiO layer, is formed. With progress of time, the scale will consist of an outer intermixed oxide + sulfide layer, and a continuous sulfide layer at the scale-metal interface. For corrosion in air + 1.1% S_2O_2, in addition to the intermixed oxide + sulfide layer formed beneath the melt, the morphology also shows a layered type of scale, consisting of sulfides beneath an oxide layer, and the layered scale is observed to be present just beneath the intermixed oxide + sulfide scale (Figure 6). It is believed that the layered scale, observed beneath the intermixed oxide plus sulfide scale, must have been originally a sulfide layer. The above scale morphology can be developed beneath the melt, only if the melt is present as a continuous layer, so that an atmosphere of high SO_3/O_2 ratio can be generated beneath the melt. However, with time, the melt

also penetrates through small pores in the oxide + sulfide layer and now the melt is present only inside the pores in the scale. In the absence of a continuous layer of the melt, the ambient atmosphere has direct access to the oxide and sulfide. Therefore, the sulfides will oxidize to form a NiO layer, and thus, a layered scale is formed beneath the intermixed oxide + sulfide scale. Some of the sulfides in outer intermixed scale are also oxidized. The pores are randomly distributed in the scale and because of this, some isolated pockets may not come in contact with the ambient atmosphere, thus, preserving the sulfides in the intermixed scale. Indeed, the sulfides in the intermixed scale are only observed inside isolated pockets.

Further degradation of the metal proceeds by a sulfidation-oxidation mechanism, as described by Spengler and Viswanathan (29), and Stringer, et al. (30), in which the sulfur, released by the oxidation of sulfides diffuses into the metal. Thus, more sulfides are formed inside the metal. The oxidation of the sulfides produces a porous oxide scale, through which the oxidizing gases can diffuse and reach the sulfide surface again, thus, the process is repeated. Spengler and Viswanathan (29) observed that the total sulfur in the metal is conserved, which leads to the continuous degradation of the metal.

For corrosion in an atmosphere consisting of air + 0.104% SO_2, it was indicated earlier that decomposition of the melt takes place at the oxide-metal interface. The scale morphology in Figure 15 suggests that the partial decomposition of the melt takes place at an early stage of the degradation process. The decomposition of the melt at the oxide-melt interface leads to a layer of Ni_2O_3. It

appears that once a layer of Ni_2O_3 is established a layer consisting of oxides + sulfide mixture cannot be developed, presumably because of the continuous evolution of O_2 due to the conversion of Ni_2O_3 to NiO. It is known that with an increase in SO_3/O_2 or SO_2/O_2 ratio, the scale morphology changes from a mixed oxide + sulfide scale to a layered type of scale, consisting of sulfides beneath an oxide layer (28). Thus, a layered type of scale, consisting of sulfides beneath an oxide layer will be developed. With progress of time, the rest of the melt penetrates through the pores in the scale, and further degradation proceeds by the sulfidation-oxidation mechanism, as has been described earlier.

The formation of sulfides in the metal appears to be the major factor in the degradation mechanism for nickel. For oxidation of nickel in a gas mixture consisting of air + 1.1% SO_2 or air + 0.104% SO_2, and without the presence of Na_2SO_4, the sulfides can also be formed in the scale. For oxidation in gas mixtures consisting of air + SO_2, the extent of sulfide formation is known to increase with an increase in the SO_2/O_2 ratio of the atmosphere. In the present experiments, the level of SO_2 in the atmosphere is relatively small, thus, the amount of sulfides in the scale would also be small. Therefore, in the absence of Na_2SO_4, the scale would be relatively protective. The presence of Na_2SO_4, clearly facilitates the formation of large amount of sulfides, by forming a Na_2SO_4-$NiSO_4$ melt, through which only SO_3 can be transported.

b. Corrosion Behavior at 923°C

At 923°C, Na_2SO_4 is molten, thus, the oxidation of nickel takes

place in the presence of a melt from the very beginning. The oxidation of nickel takes place by transport of the oxidzing gases through the Na_2SO_4 melt, and it was indicated earlier that SO_3 is the principal oxidizing species because of its high solubility in the melt. At the salt-metal interface, if the rate of oxidation of nickel is higher than the rate of transport of SO_3 through the melt, a SO_3 gradient is established through the melt. Depending on the SO_2+SO_3 level of the ambient and the thickness of the melt, at the salt-oxide interface, two modes of dissolution of NiO in the melt are possible.

(1) In the Na_2SO_4 melt, the Na_2O activity and P_{SO_3} are related by the equilibrium conditions for the reaction:

$$Na_2SO_4(\ell) = Na_2O(\ell) + SO_3(g) \qquad [2]$$

Any decrease in P_{SO_3} results in an increase in the Na_2O activity of the melt. Gupta and Rapp (31) have measured the solubility of NiO in Na_2SO_4 melt as a function of Na_2O activity at 1200K; their solubility curve is shown in Figure 18. At certain a_{Na_2O} in the liquid, a solubility minimum is obtained. If the P_{SO_3} in the ambient atmosphere is low, then the oxidation of nickel beneath the melt may reduce the P_{SO_3} and increase the a_{Na_2O} at the salt-oxide interface to a level, where basic dissolution of NiO is possible. The reprecipitation of these dissolved species requires the presence of a solubility gradient across the melt (32). When the basic dissolution of oxides take place at the salt-oxide interface, and the ambient atmosphere contains SO_3, a large solubility gradient can be established across the melt as compared to a situation where the ambient atmosphere does not contain any SO_3. Thus, due to this large solubility gradient, a thick

precipitated zone of oxides will be produced.

(2) At high $P_{SO_2} + P_{SO_3}$ in the ambient atmosphere, an SO_3 gradient is again established across the melt. However, the P_{SO_3} at the salt-oxide interface does not fall to a value, where basic dissolution of the oxide is possible. Instead, the dissolution is acidic, and NiO dissolves in the melt as Ni^{++}. For the case of acidic dissolution at the salt-oxide interface, Rapp (32) has proposed a model, in which the continuous dissolution and reprecipitation of the metal oxide take place due to the presence of a solubility gradient across the melt. According to Rapp's (32) proposed model, M dissolves at the oxide-melt interface as M^{++} when the atmosphere above the melt contains $SO_3(g)$. Then, at the salt-gas interface, M^{++} ions are converted to M^{+++} by reaction with $O_2(g)$:

$$2M^{++} + \frac{1}{2} O_2(g) = 2M^{+++} + O^{2-} \qquad [3]$$

Luthra and Shores (3) have proposed a similar mechanism for the corrosion of cobalt base alloys in the presence of Na_2SO_4 deposit and $SO_3(g)$ in the atmosphere, in which cobalt oxides dissolve as Co^{++} at the salt-oxide interface, and the salt-gas interface, the dissolved oxides are reprecipitated as Co_3O_4.

In the present experiments, when the atmosphere contains 0.104% SO_2, the scale morphology suggests that during the initial stages of corrosion, the dissolution at the salt-oxide interface is basic in nature. Thus, a thick, outer , porous NiO layer is produced due to the dissolution-reprecipitation process. The magnitude of the SO_3 gradient across the melt, generated because of SO_3 consumption by the oxidation of nickel, increases with an increase in the thickness of the melt. Thus, for a thick melt, the amount of Na_2O generated at the

oxide-salt interface is large, and leads to the dissolution of larger amounts of oxide before the a_{Na_2O} or P_{SO_3} equalize throughout the melt. This readily explains the increase in the thickness of the outer porous NiO layer with an increase in the thickness of the melt.

For corrosion experiments in the presence of a gas mixture consisting of air + 1% SO_2, the scale morphology showed a strong dependence on the thickness of the melt. For example, when the total of Na_2SO_4 deposit was only 0.01 mg/cm^2, the scale morphology showed an outer porous NiO + Ni_2O_3 layer. For such a small amount of the Na_2SO_4 deposit, the thickness of the melt is extremely small, thus, any SO_3 consumed due to the oxidation of nickel can be easily replenished by diffusion through the melt. Under these circumstances acidic dissolution of NiO was possible. The outer porous NiO + Ni_2O_3 layer is due to conversion of Ni^{++} ions to Ni^{+++} ions at the salt-gas interface. When the amount of the Na_2SO_4 deposit increased to 1.5 mg/cm^2, the thickness of the deposit increases. Thus, a large SO_3 gradient is established across the melt, which makes the basic dissolution of the oxide possible; and a thick outer porous NiO layer is developed.

In atmospheres containing 10% SO_2, the SO_3 content is relatively high. Therefore, irrespective of the thickness of the melt, the P_{SO_3} at the salt-oxide interface does not fall to a point, where basic dissolution of the oxide is possible. Instead, at all times, the dissolution is acidic and during the initial stage of corrosion, the outer precipitated layer consists of Ni_2O_3.

During the initial stages of corrosion, the degradation of nickel appears to be via a dissolution - reprecipitation process. However, the melt gradually penetrates the oxide and reaches the metal surface.

In the case of basic fluxing, the dissolution is due to a high Na_2O activity at the salt-oxide interface. However, gradually, because of the dissolution, the P_{SO_3} becomes equal throughout the melt and now a Na_2SO_4-$NiSO_4$ melt is formed. Thus, whether the dissolution is acidic or basic, the final composition of the melt is a mixture of Na_2SO_4 + $NiSO_4$. Addition of $NiSO_4$ to Na_2SO_4 lowers the melting point of the melt, decreasing its viscosity and making it easier for the melt to penetrate through the oxide. Further oxidation of nickel takes place beneath the melt, the oxidants being supplied by the decomposition of the Na_2SO_4-$NiSO_4$ melt. This mechanism has been described earlier for corrosion at 750°C, when the atmosphere contained 0.104% SO_2 in air.

5. SUMMARY AND CONCLUSION

Based on the experimental results and discussion, a generalized model for the corrosion of nickel, in the presence of Na_2SO_4 deposit and $SO_3(g)$ in the atmosphere, can be described. The sequence of steps leading to the degradation of nickel at temperatures below the melting point of Na_2SO_4 are described below:

(1) A Na_2SO_4-$NiSO_4$ melt is formed.

(2) Melt penetrates the outer oxide layer and reaches the metal surface.

(3) The oxidation of metal now takes place beneath the melt, and sulfides are formed. Depending on the SO_2 content of the atmosphere, the scale morphology can be either of these two types:

(a) an intermixed oxide + sulfide scale and a layer of sulfide layer at the scale-metal interface (formed at

low SO_2 content).

For an atmosphere containing low levels of SO_2, the melt at the oxide-melt interface decomposes.

(4) The melt further penetrates the pores in the oxide or oxide + sulfide layer, and the scale is in contace with the ambient atmosphere. The sulfides are oxidized, thus, releasing further sulfur into the metal. The metal continues to degrade by the sulfidation-oxidation mechanism.

At temperatures above the melting point of Na_2SO_4, during the initial stage of corrosion, the degradation is by a dissolution - reprecipitation mechanism. The nature of the dissolution and reprecipitation process is dependent on the SO_2-SO_3 level in the atmosphere and the thickness of the Na_2SO_4 melt. The dissolution is acidic for high SO_2 level in the atmosphere and a thin melt; basic for low SO_2 level and a thick melt. After the initial stage, the degradation proceeds by penetration of the melt through the oxide, and decomposition of the melt to supply the oxidants necessary for the oxidation.

ACKNOWLEDGEMENT

This work was supported by the Director, Office of Energy Research, Office of Basic Energy Sciences, Materials Sciences Division of the U.S. Department of Energy under Contract Number DE-AC03-76SF00098.

REFERENCES

1. D. J. Wortman, R. E. Fryxell and I. J. Bessen, in "Proceedings of the 3rd Conference on Gas Turbine Materials in a Marine Environment," held at U. of Bath, England, September 1976, Session V, Paper 11.

2. K. L. Luthra and D. A. Shores, J. Electrochemical Society, 127, 2202 (1980).

3. D. A. Shores and K. L. Luthra, Final Report on "Study of Mechanism of Hot Corrosion in Environments Containing NaCl," GE Report Number SRD-80-011, November 1979.

4. R. L. Jones, N.R.L. Memorandum Report 4409 (November 1980).

5. R. L. Jones and S. T. Gadomski, Paper presented at Electrochemical Society Meeting, Denver, Colorado, October 11-16, 1981.

6. J. A. Goebel, F. S. Pettit and G. W. Goward, Metall. Trans. 4, 261 (1973).

7. P. Kofstad and A. Åkesson, Oxidation of Metals, 14, 301 (1980).

8. R. E. Andersen, J. Electrochem. Soc., 126, 328 (1979).

9. L. P. Kostin, L. L. Pluzbnikov and A. N. Ketov, Russian J. of Physical Chemistry, 49, 1313 (1975).

10. A. J. B. Cutler and C. J. Grant in "Metal-Slag-Gas Reactions and Processes" edited by W. W. Smeltzer and Z. A. Foroulis, Electrochem. Soc., Princeton (1975) p. 591.

11. A. K. Misra, D. P. Whittle and W. L. Worrell. Accepted for publication in J. Electrochem. Soc.

12. W. W. Smeltzer and D. J. Young in "Progress in Solid State Chemistry," vol. 10, Part 1, p. 17-54 (1975).

13. J. A. Goebel and F. S. Pettit, Metall. Trans. 1, 1943 (1974).

14. P. Kofstad, Oxidation of Metals and Alloys.

15. G. B. Gibbs and R. Hales, Corrosion Science, 7, 487 (1977).

16. R. Hales, R. E. Smallman and P. S. Dobson, Proc. R. Soc., 71, A307 (1968).

17. J. Stringer, Metals Soc. Conf. Proc. Vacancies 76, p. 187, Bristol (1976).

18. R. Hales and A. C. Hill, Corrosion Science, 12, 843 (1972).

19. S. Mrowec, Corrosion Science, 7, 563 (1967).

20. C. B. Alcock and M. G. Hocking, Trans. Inst. Min. Metall. (Sect. C), 75, C27, (1966).

21. C. B. Alcock, M. G. Hocking and S. Zadar, Corrosion Science, 9, 111, (1969).

22. M. C. B. Hotz and T. R. Ingraham, Can. Met. Quart., 4, 295 (1965).

23. H. Hindam, Private Communication.

24. M. C. Pope and N. Birks, Oxidation of Metals, 12, 1973 (1978).

25. A. Rahmel, Oxidation of Metals, 9, 401 (1975).

26. P. Kofstad and G. Åkesson, Oxidation of Metals, 12, 503 (1978).

27. K. L. Luthra and W. L. Worrell, Metall. Trans., 10A, 621 (1979).

28. C. S. Giggins and F. S. Pettit, Oxidation of Metals, 14, 363 (1980).

29. C. J. Spengler and R. Viswanathan, Metall. Trans., 3, 161 (1972).

30. M. E. El Dahshan, D. P. Whittle and J. Stringer, Oxidation of Metals, 8, 179 (1974).

31. D. K. Gupta and R. A. Rapp, J. Electrochem. Soc., 127, 2194 (1980).

32. R. A. Rapp and K. S. Goto, "The Hot Corrosion of Metals by Molten Salts," in Proc. 2nd Int. Symp. Molten Salts, J. Braunstein Ed., Electrochemical Society, Princeton (1979).

TABLE 1

X-ray Diffraction Data for the Corrosion Product of Nickel, Coated with 1.5 mg/cm^2 Na_2SO_4 and Oxidized for 60 hours in an Atmosphere Consisting of Air + 0.104% SO_2 (P_{SO_3} = 6.8 x 10^{-4} atm.)

(Only the Main Lines are Shown)

d Spacing A°	Compound
1.512	Na_2SO_4
2.325	Na_2SO_4
2.614	Na_2SO_4
2.798	Na_2SO_4
1.472	NiO
2.076	NiO
2.391	NiO
1.762	Ni_2O_3
2.011	Ni_2O_3
2.796	Ni_2O_3
1.653	Ni_3S_2
1.82	Ni_3S_2
2.866	Ni_3S_2
4.089	Ni_3S_2

FIGURE CAPTIONS

1. Kinetics of sulfation of NiO powders in the presence of Na_2SO_4.
2. Test for diffusion controlled kinetics for the sulfation reaction after the formation of the melt.
3. (a) Kinetics of corrosion of nickel coated with 1.5 mg/cm^2 Na_2SO_4 and exposed at 750°C to an atmosphere consisting of air + SO_2 + SO_3.

   (b) Same as above, but for longer times.
4. Kinetics of corrosion of nickel, coated with 1.5 mg/cm^2 Na_2SO_4 and exposed to an atmosphere consisting of air + SO_2 + SO_3 at 923°C.
5. Cross-section of nickel, coated with 1.5 mg/cm^2 Na_2SO_4 and oxidized for 30 minutes in an atmosphere consisting of air + 1.1% SO_2 (P_{SO_3} = 7.28 x 10^{-3} atm.)

   (a) showing grain boundary penetration

   (b) same as a, but at higher magnification

   (c) showing void formation at metal grain boundaries.
6. (a) Cross-section of nickel, coated with 1.5 mg/cm^2 Na_2SO_4 and oxidized for 2 hours in an atmosphere consisting of air + 1.1% SO_2 (P_{SO_3} = 7.28 x 10^{-3} atm.)

   (b) details of the outermost oxide layer.

   (c) details of the intermixed oxide + sulfide scale (while particles are sulfides.
7. (a) Cross-section of nickel, coated with 1.5 mg/cm^2 Na_2SO_4 and oxidized for 26 hours in an atmosphere consisting of air + 0.104% SO_2 (P_{SO_3} = 6.8 x 10^{-4} atm.)

   (b) Details of the interface of a.
8. Cross-section of nickel, coated with 1.5 mg/cm^2 Na_2SO_4 and oxidized for 60 hours in an atmosphere consisting of air + 0.104% SO_2 (P_{SO_3} = 6.8 x 10^{-4} atm.)

9. Surface of the solidified Na_2SO_4-$NiSO_4$ melt.

10. (a) Cross-section of nickel, coated with 0.55 mg/cm^2 Na_2SO_4, and exposed to an atmosphere containing 0.104% SO_2 in air for 45 minutes at 923°C.

    (b) details of the interface.

11. Cross-section of nickel, coated with 1.5 mg/cm^2 Na_2SO_4 and exposed to and atmosphere containing 0.104% SO_2 in air for 60 minutes at 923°C.

12. (a) Cross-section of nickel, coated with 0.1 mg/cm^2 Na_2SO_4 and oxidized in an atmosphere containing 1.1% SO_2 in air for 1 hour at 923°C.

    (b) details of the scale-gas interface.

13. Cross-section of nickel, coated with 1 mg/cm^2 Na_2SO_4 and oxidized in an atmosphere containing 1.1% SO_2 in air for 1 hour at 923°C.

14. Cross-section of nickel, coated with 1.5 mg/cm^2 Na_2SO_4 and oxidized in an atmosphere containing 10% SO_2 in air for 15 minutes at 923°C.

15. Cross-section of nickel, coated with 1.5 mg/cm^2 Na_2SO_4 and oxidized in an atmosphere containing 10% SO_2 in air for 45 minutes at 923°C.

16. Cross-section of nickel, coated with 1.5 mg/cm^2 Na_2SO_4 and oxidized in an atmosphere containing 10% SO_2 in air for 3 hours at 923°C.

17. Na-Ni-S-O stability diagram at 750°C.

18. Solubility of NiO in Na_2SO_4 (Gupta and Rapp).

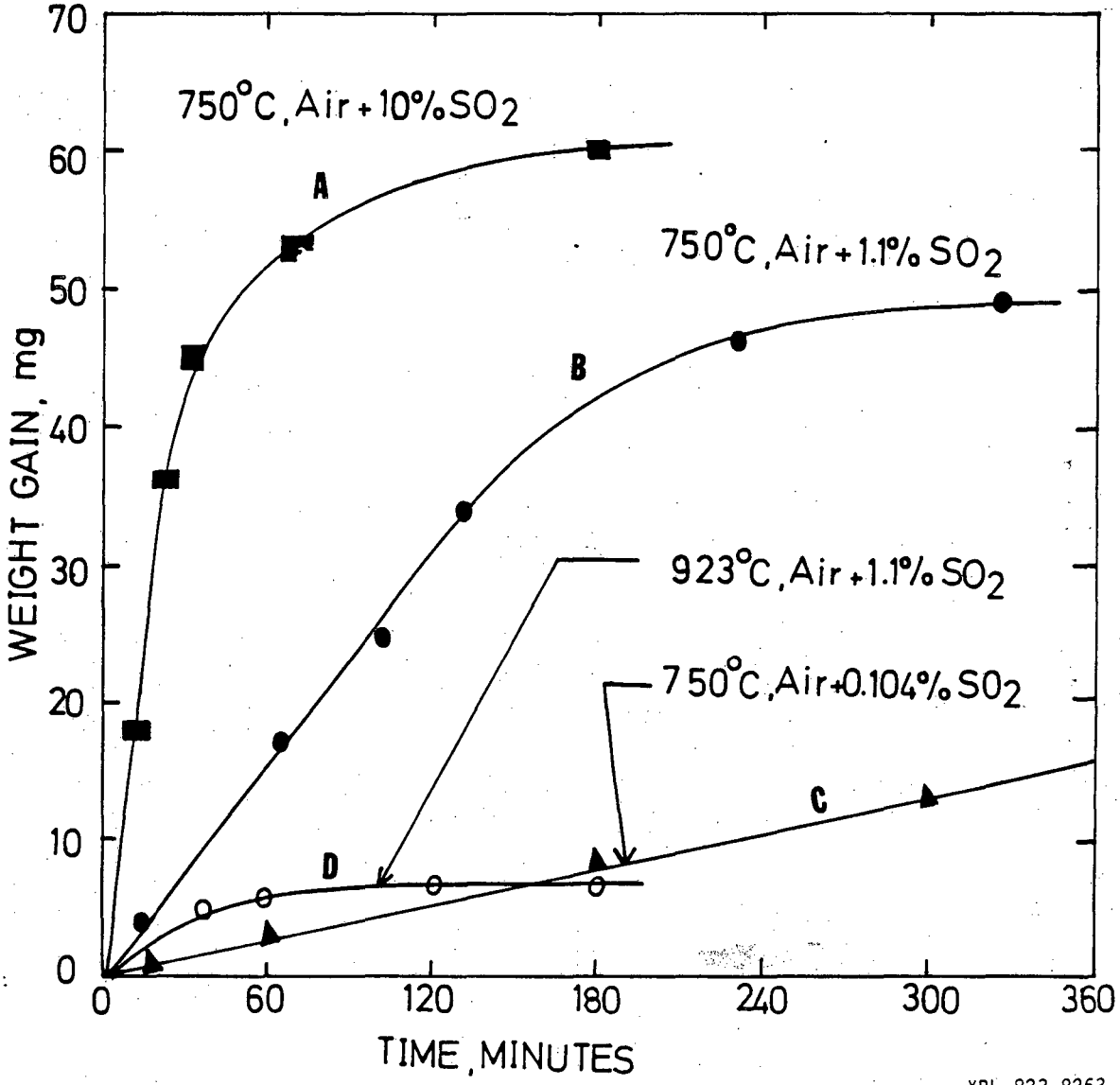

Figure 1.

XBL 823-8263

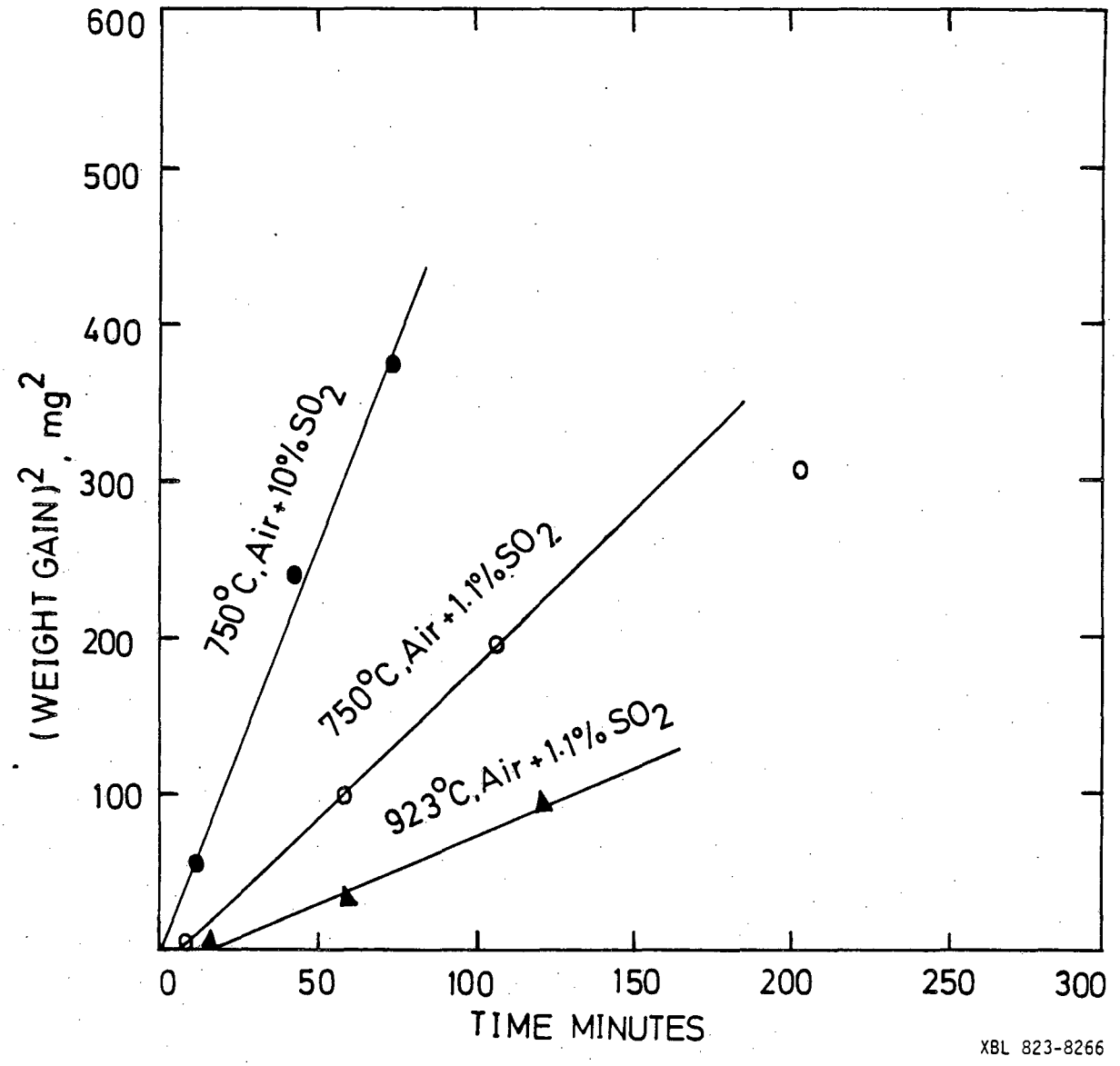
600
500
400
300
200
100
0
50
100
150
200
250
300
(WEIGHT GAIN)^2, mg^2
TIME MINUTES
750°C, Air + 10% SO_2
750°C, Air + 1.1% SO_2
923°C, Air + 1.1% SO_2
XBL 823-8266

Figure 2.

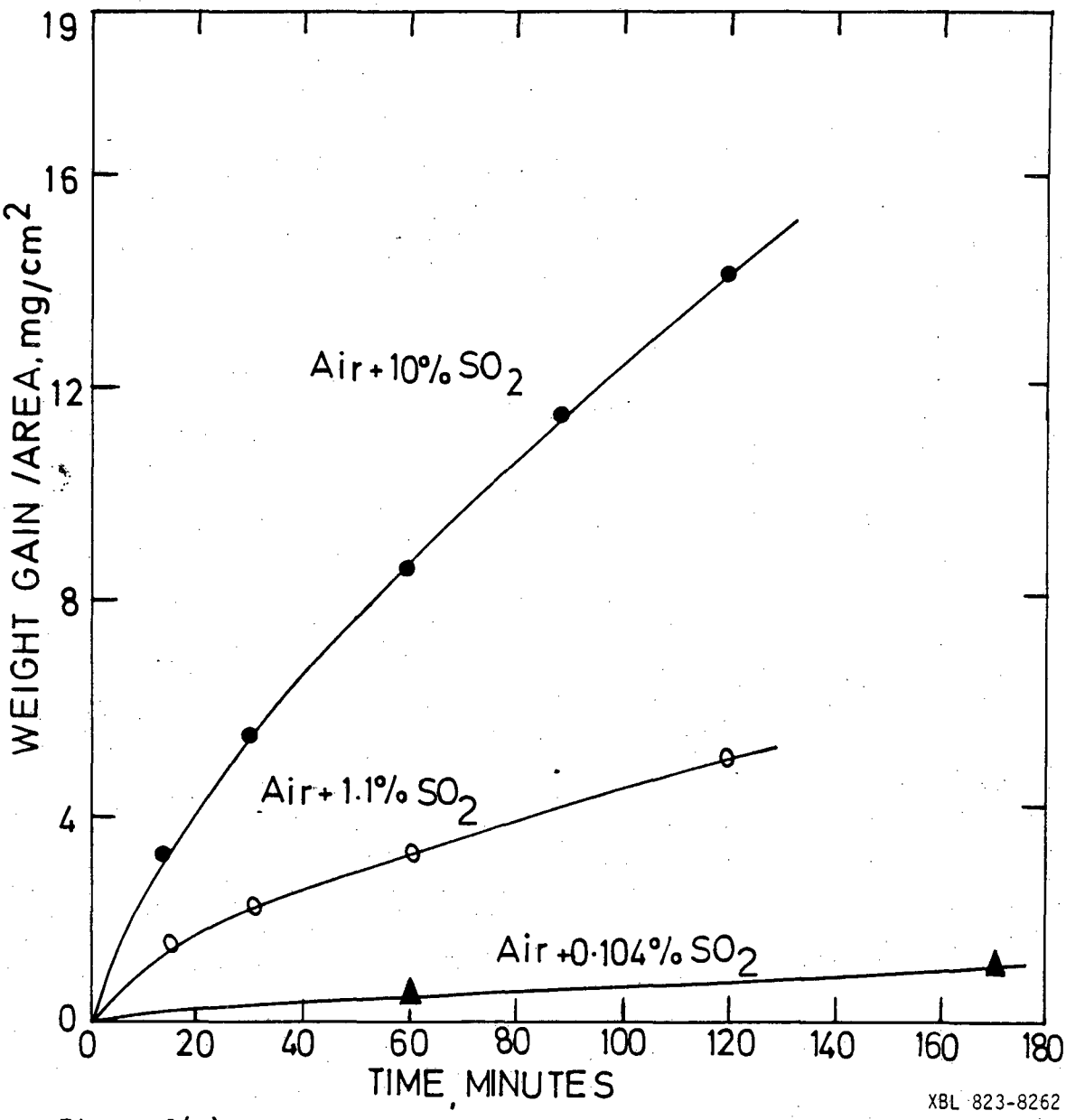
19
16
12
8
4
0
WEIGHT GAIN /AREA, mg/cm2
Air + 10% SO2
Air + 1.1% SO2
Air +0·104% SO2
0
20
40
60
80
100
120
140
160
180
TIME, MINUTES
XBL 823-8262

Figure 3(a)

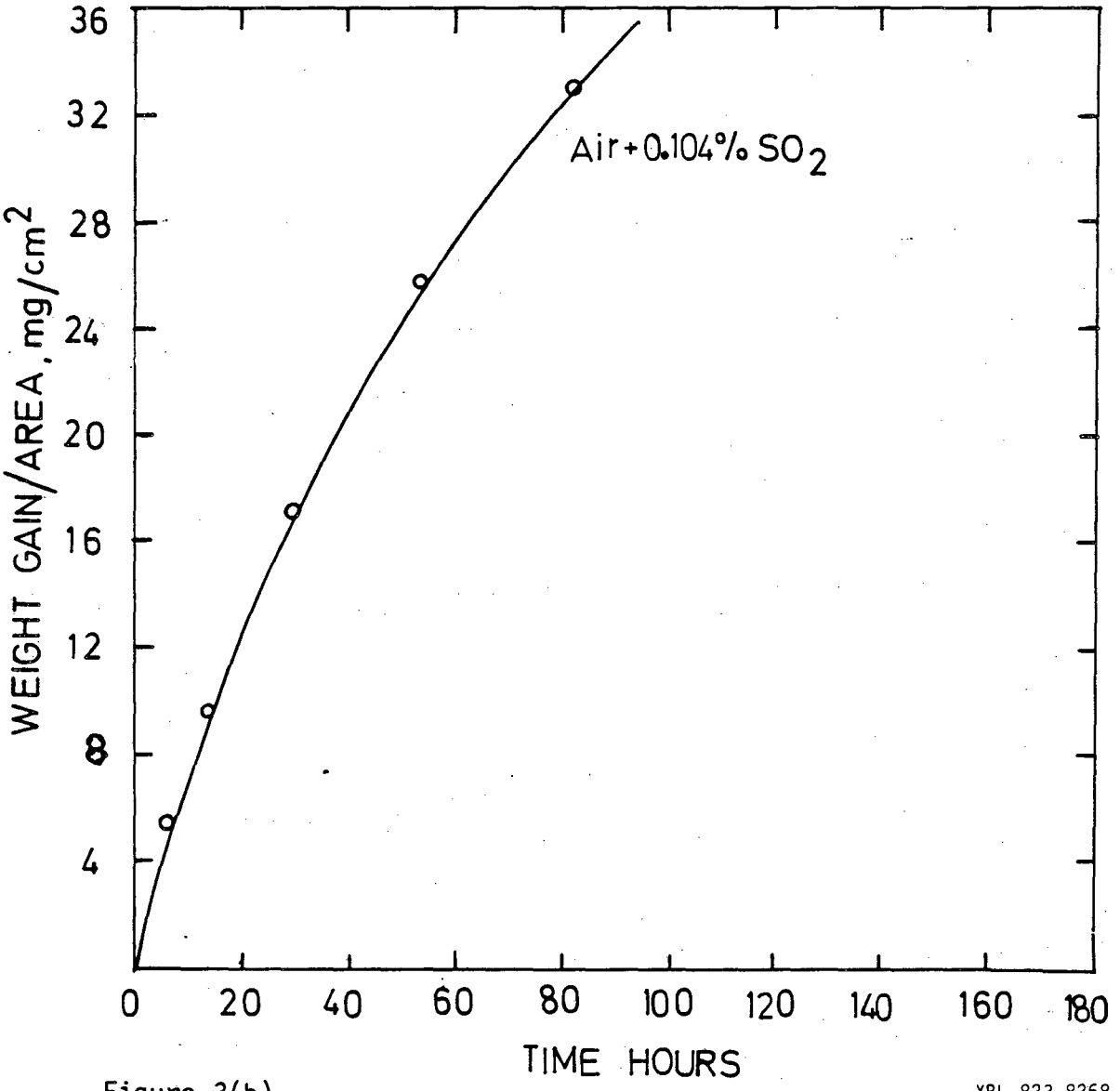

Figure 3(b)

XBL 823-8268

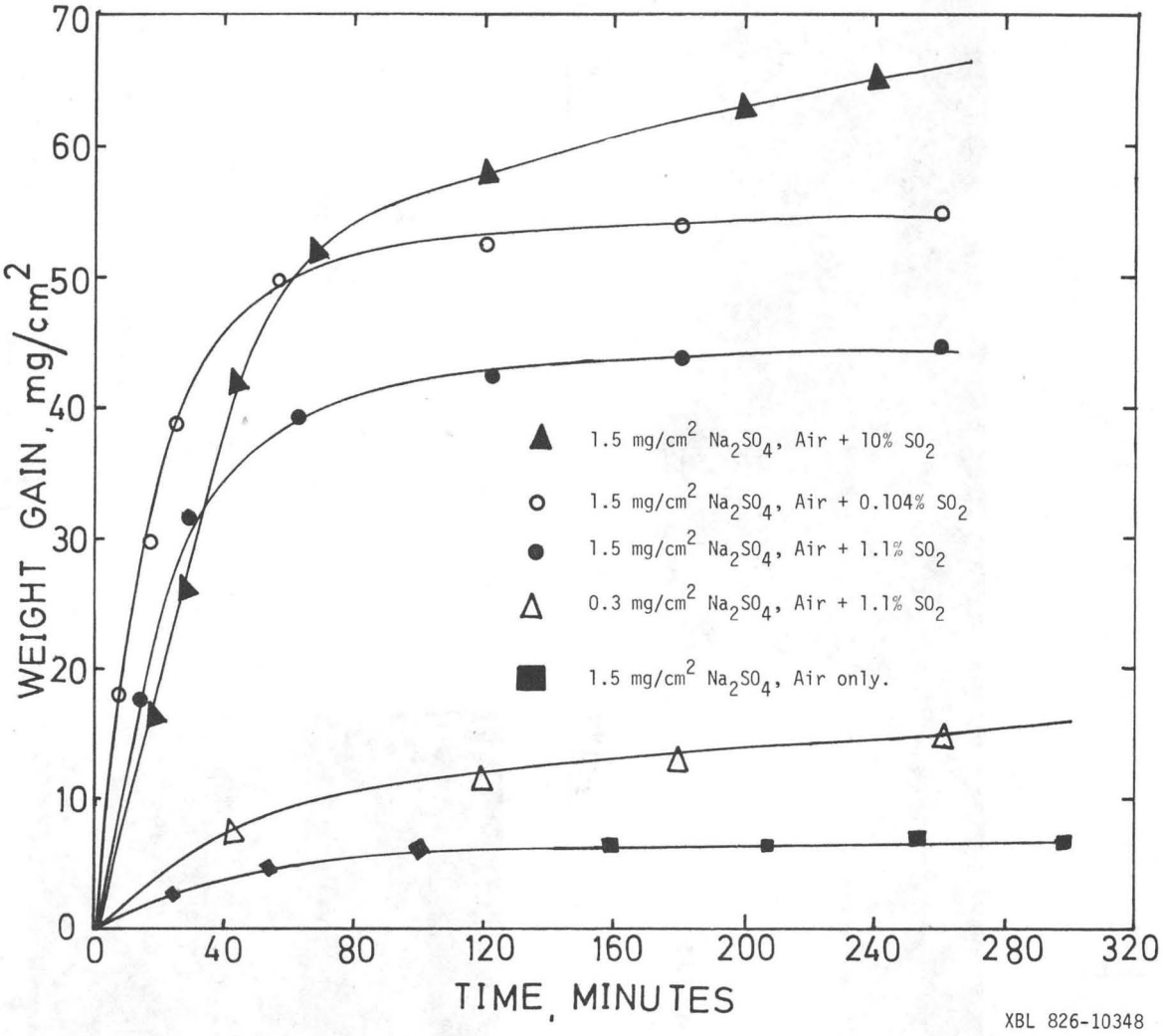
WEIGHT GAIN, mg/cm^2
TIME, MINUTES
0
10
20
30
40
50
60
70
0
40
80
120
160
200
240
280
320
1.5 mg/cm^2 Na_2SO_4, Air + 10% SO_2
1.5 mg/cm^2 Na_2SO_4, Air + 0.104% SO_2
1.5 mg/cm^2 Na_2SO_4, Air + 1.1% SO_2
0.3 mg/cm^2 Na_2SO_4, Air + 1.1% SO_2
1.5 mg/cm^2 Na_2SO_4, Air only.
XBL 826-10348

Figure 4.

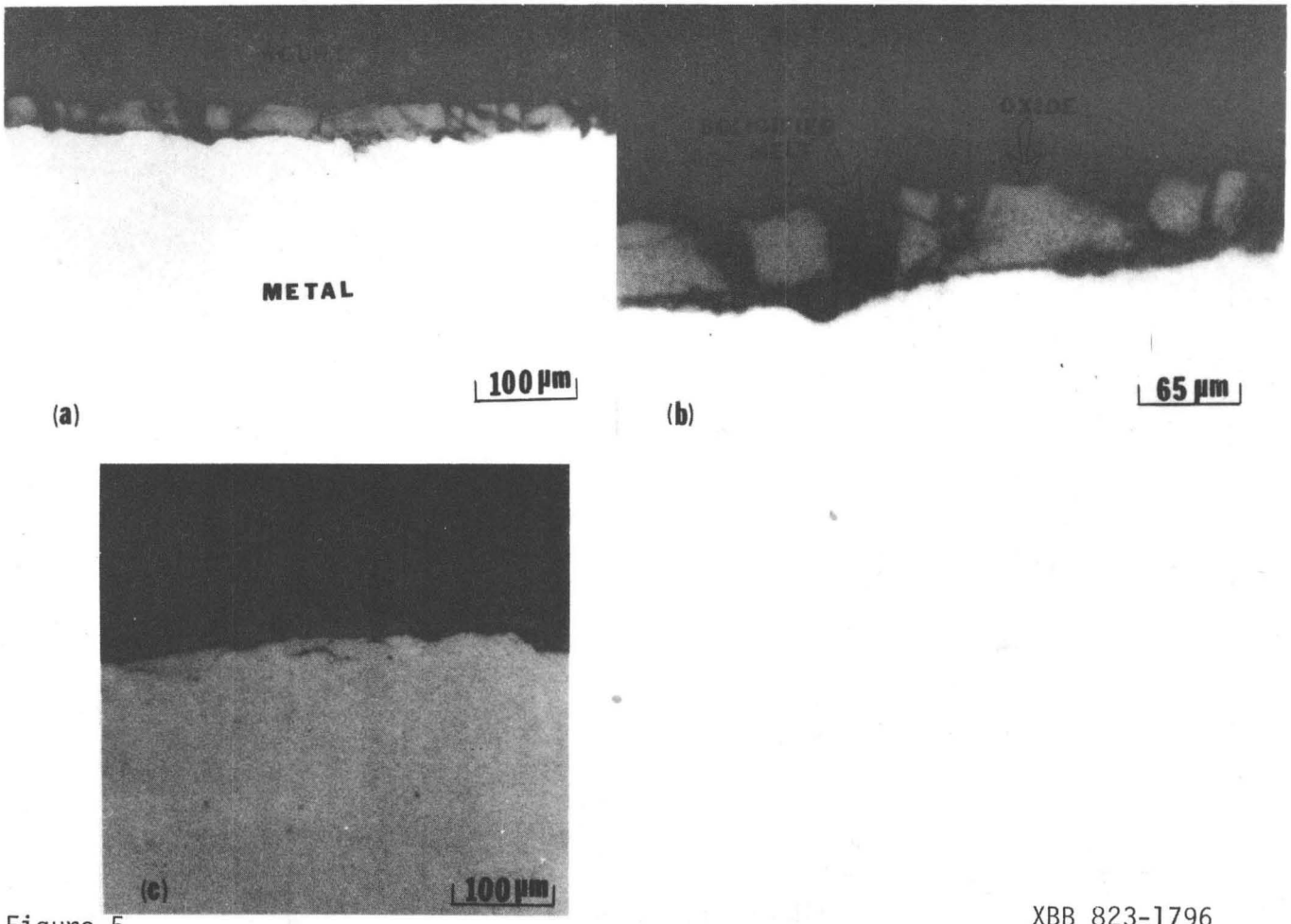

Figure 5.

XBB 823-1796

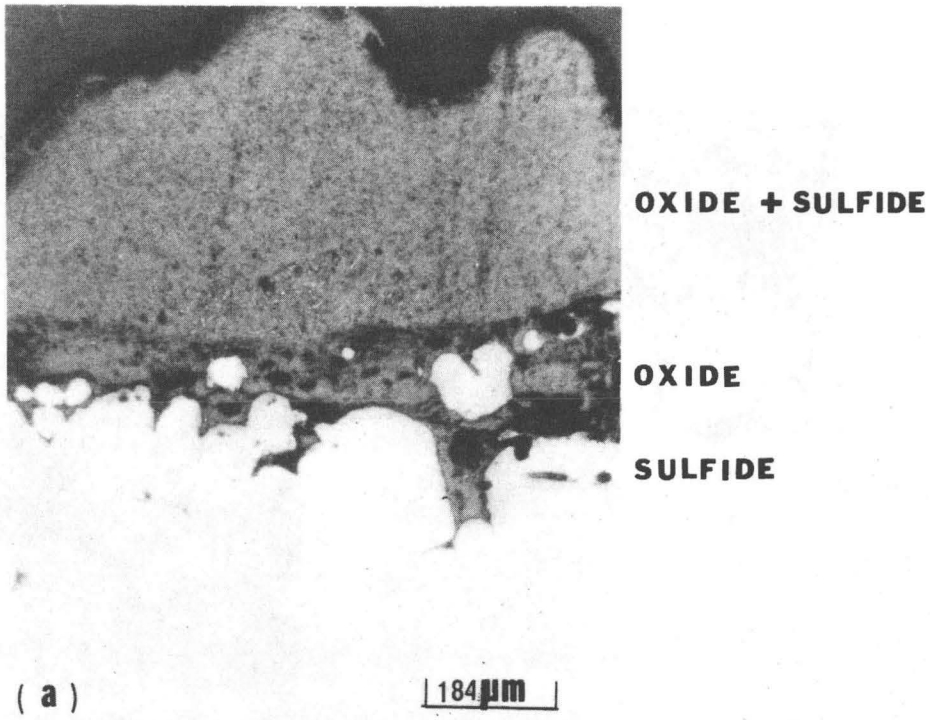

Figure 6. XBB 823-1794

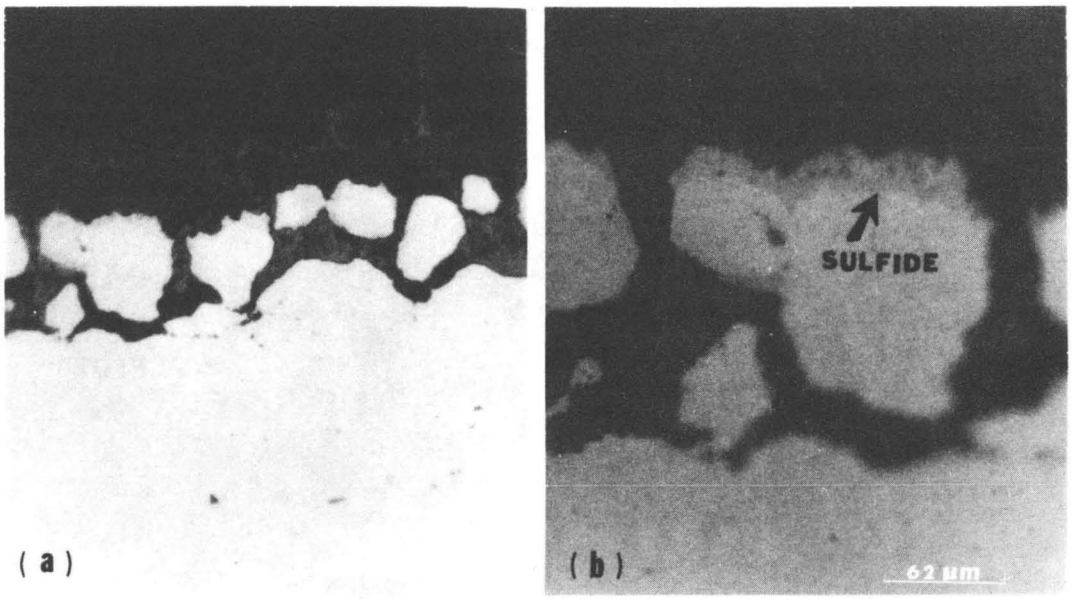

Figure 7.

XBB 823-1798

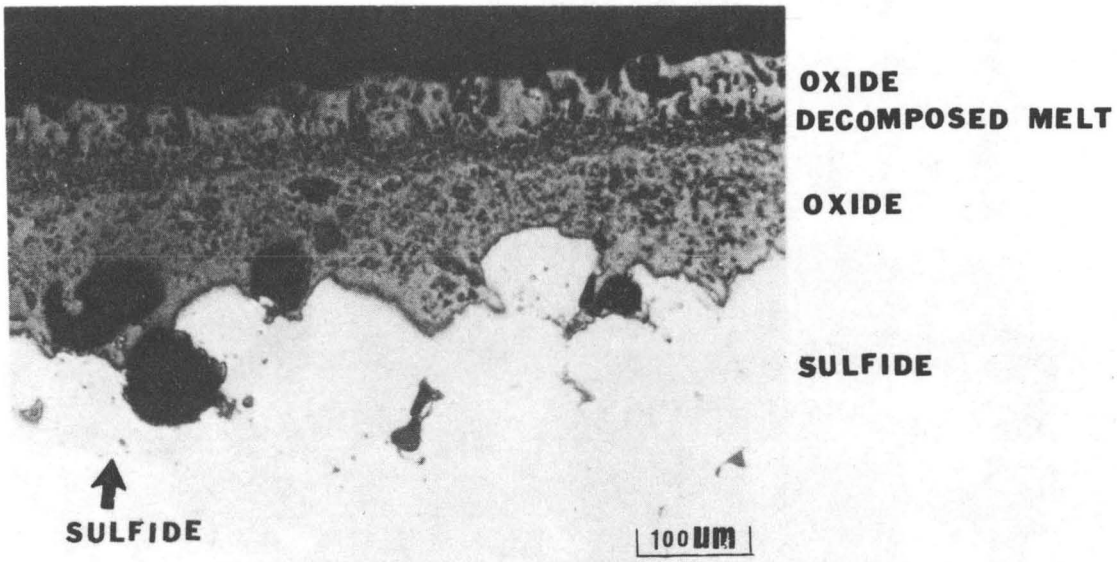

Figure 8. XBB 823-1795

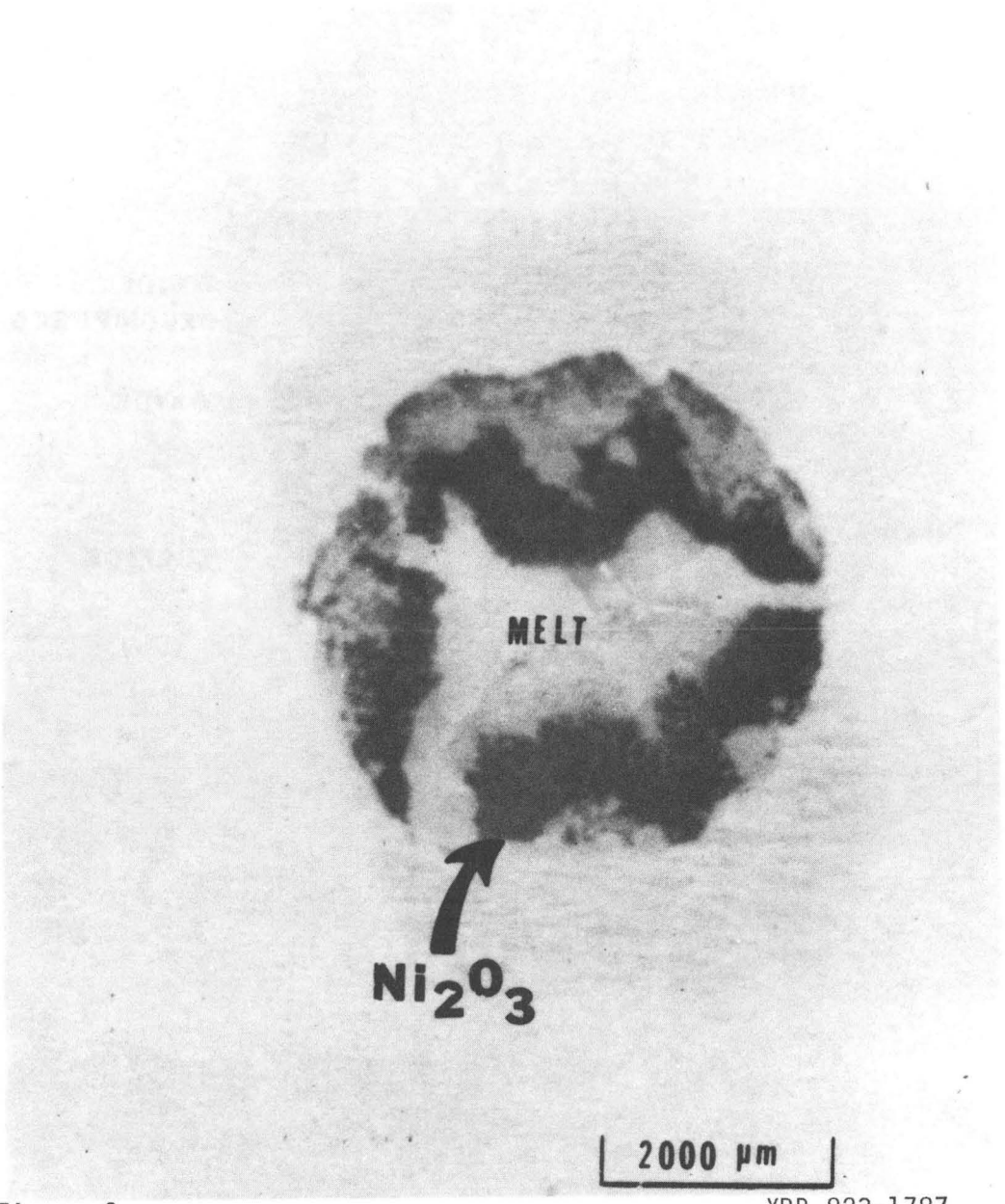

Figure 9. XBB 823-1787

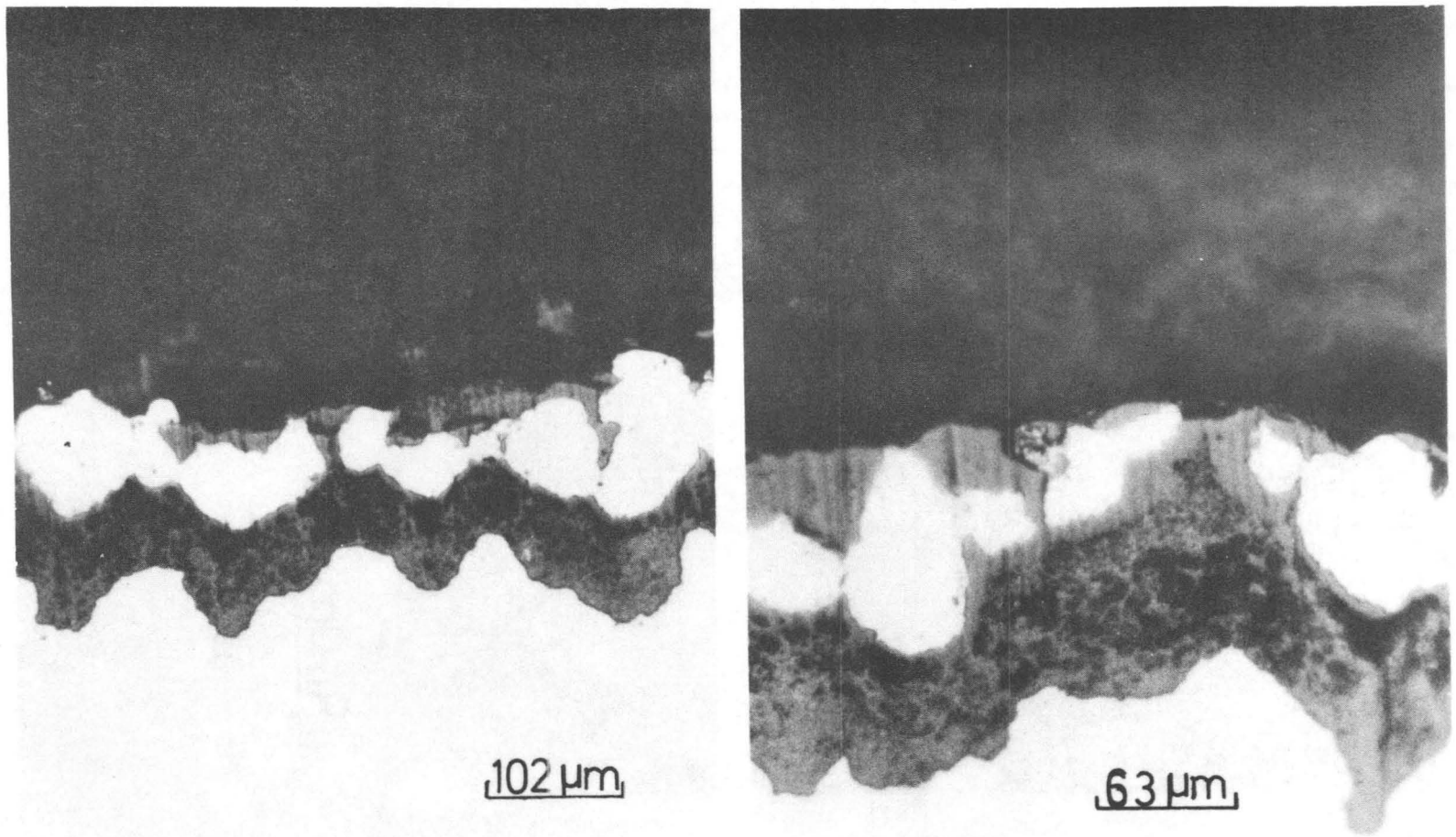

Figure 10.

XBB 826-5097

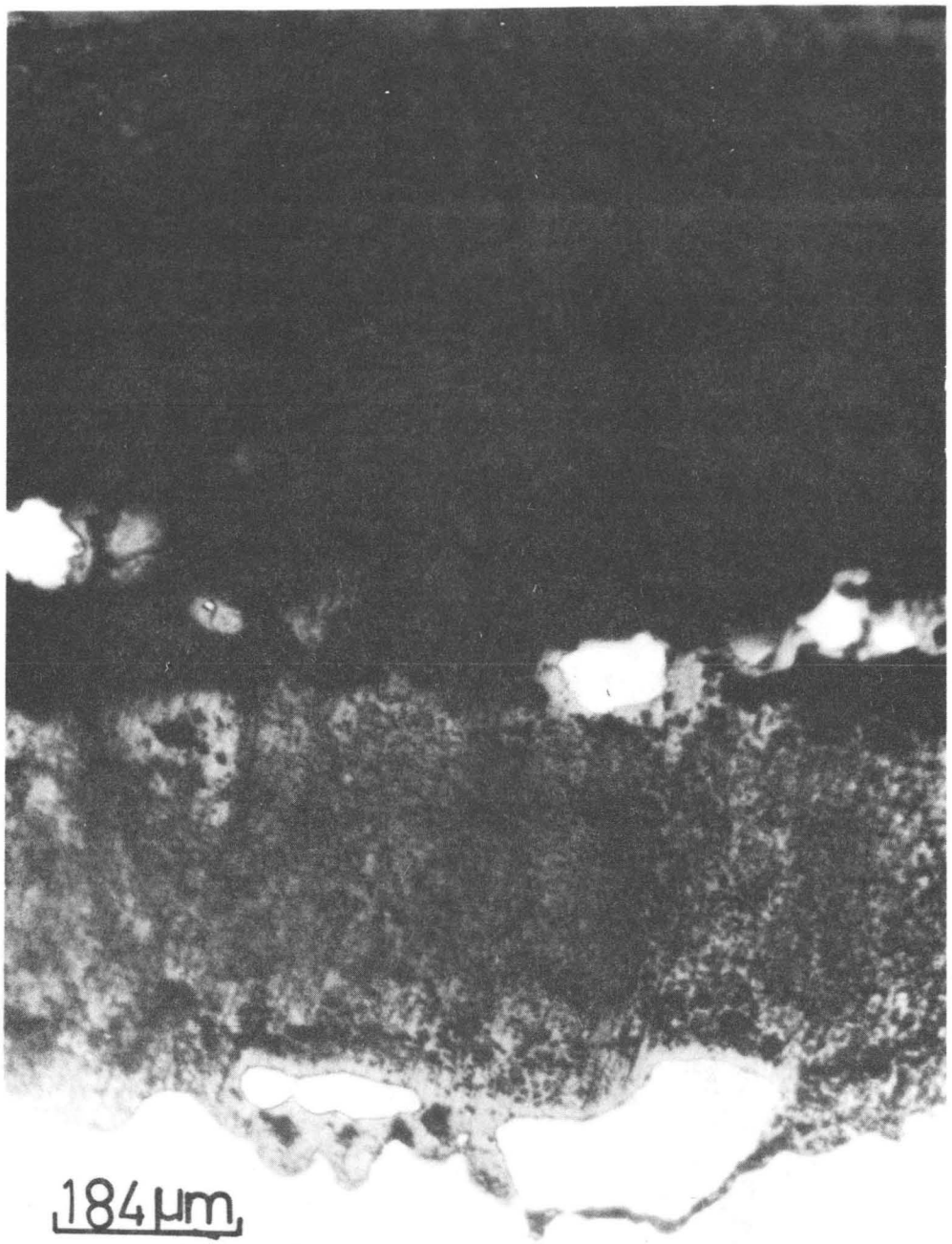

Figure 11. XBB 826-5103

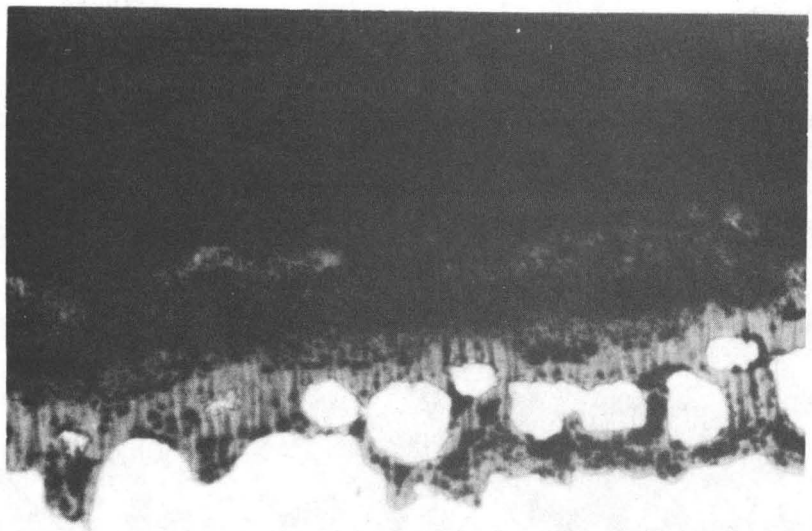

184μm

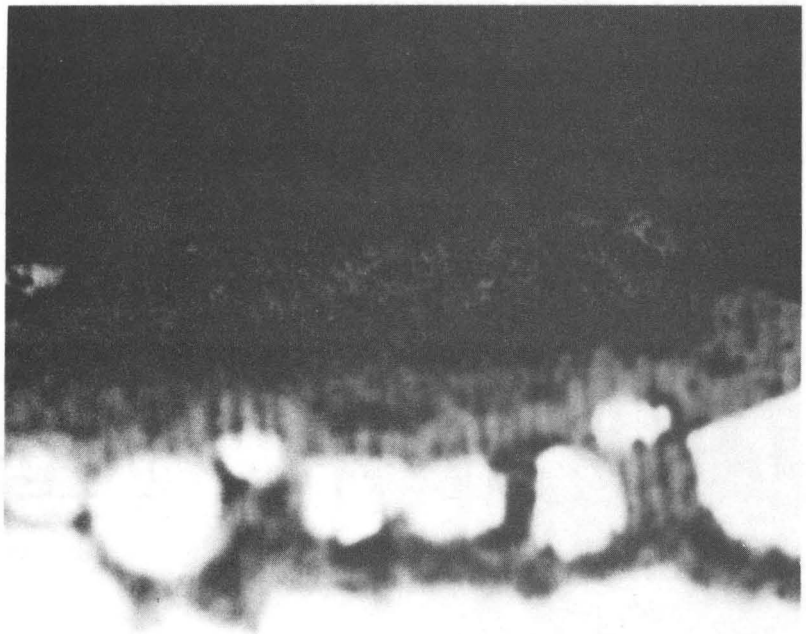

102μm

Figure 12.

XBB 826-5098

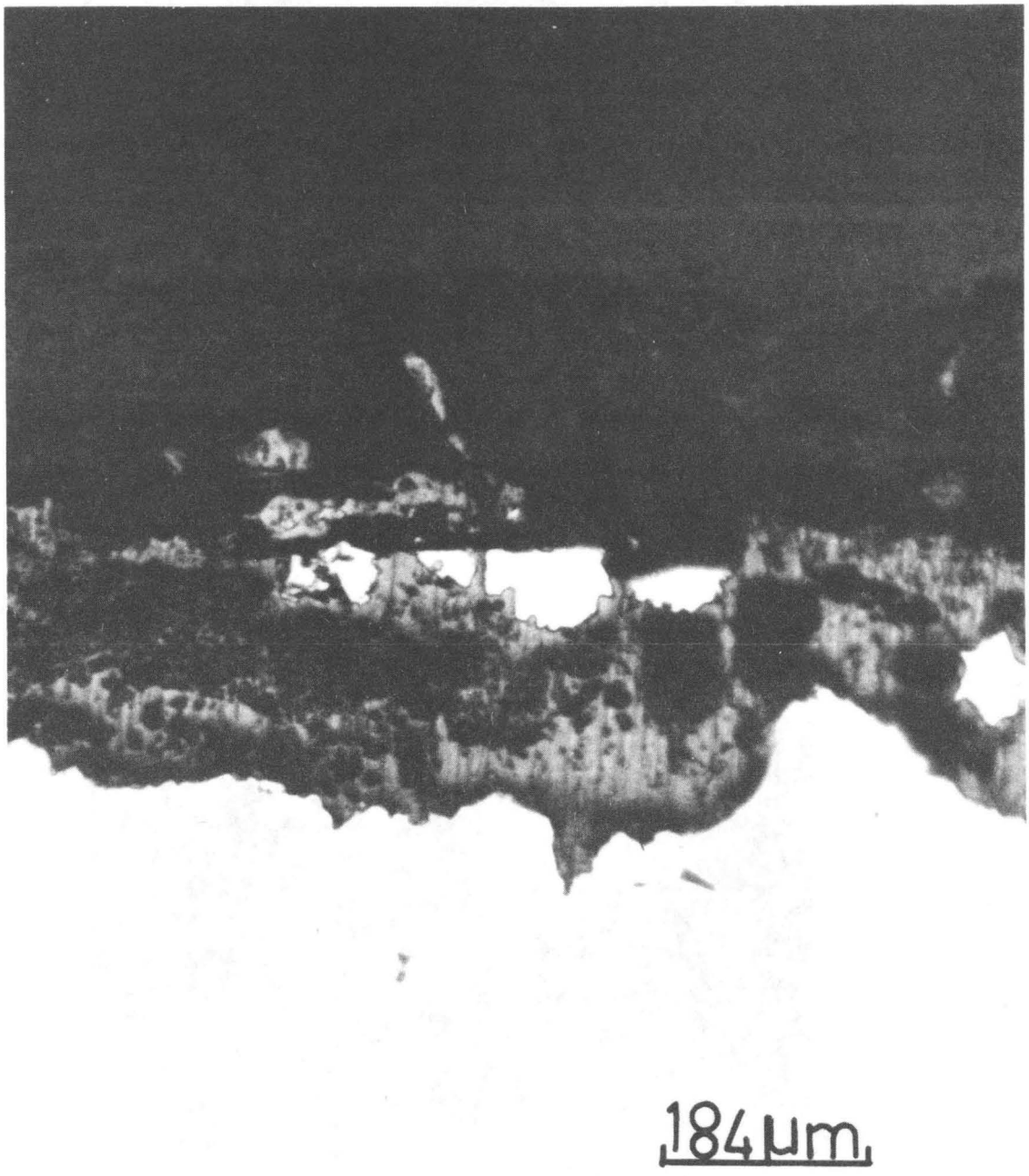

Figure 13.

XBB 826-5102

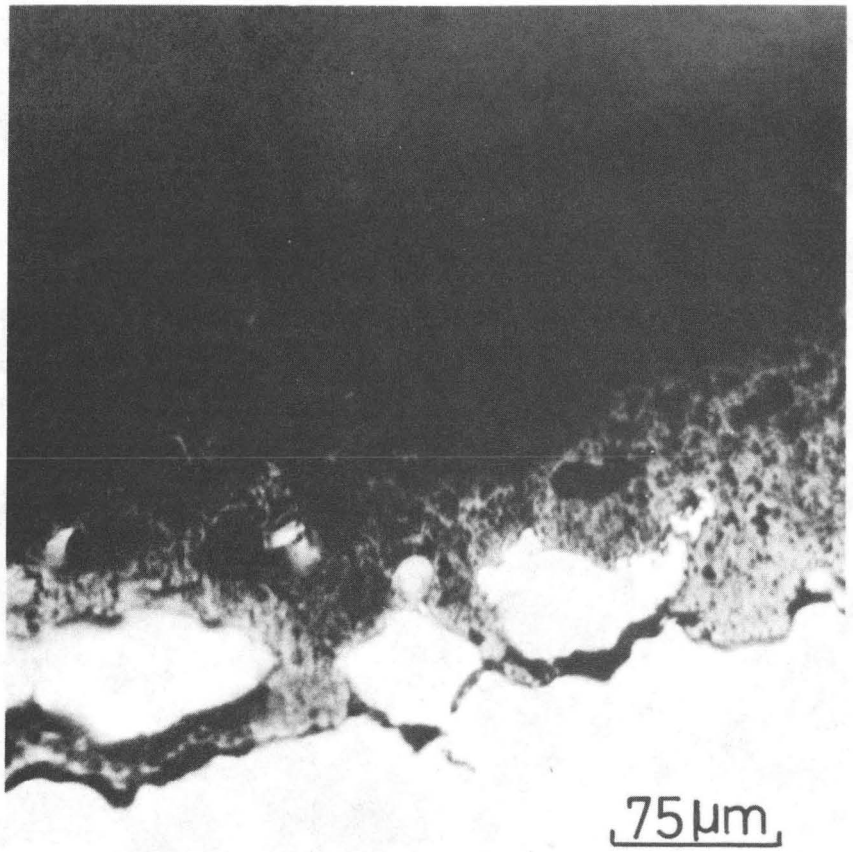

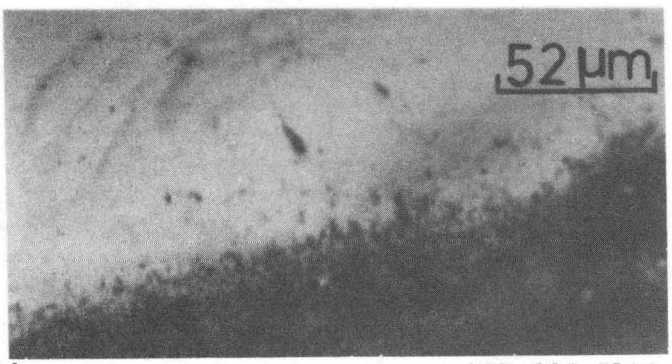

Figure 14. XBB 826-5104

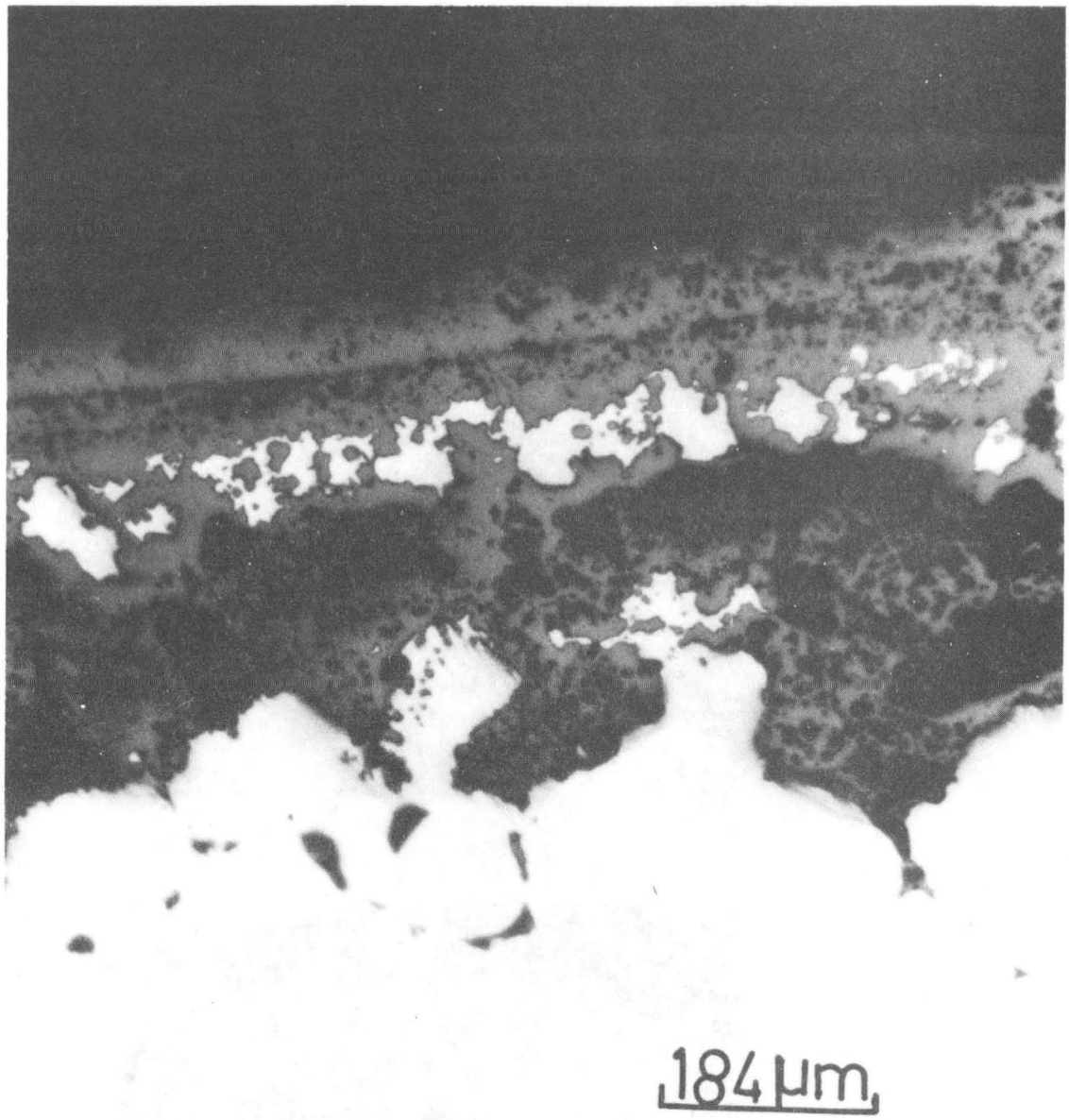

Figure 15.

XBB-826 5101

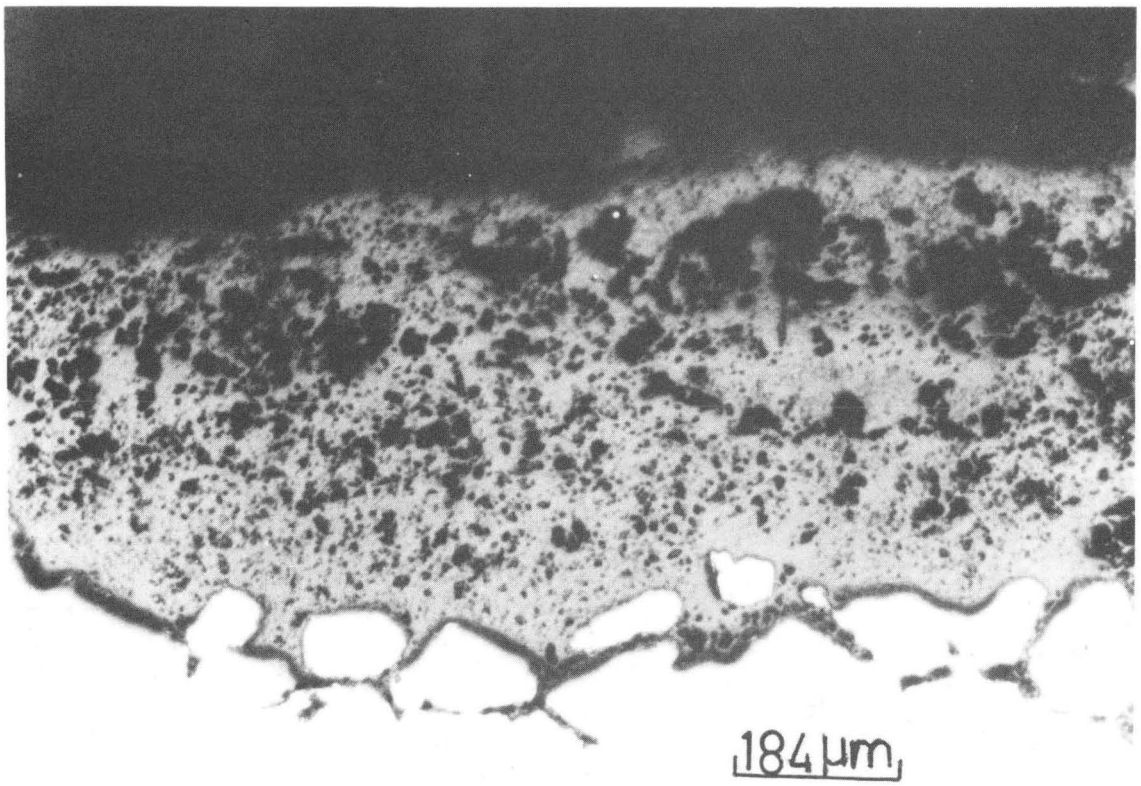

Figure 16. XBB 826-5100

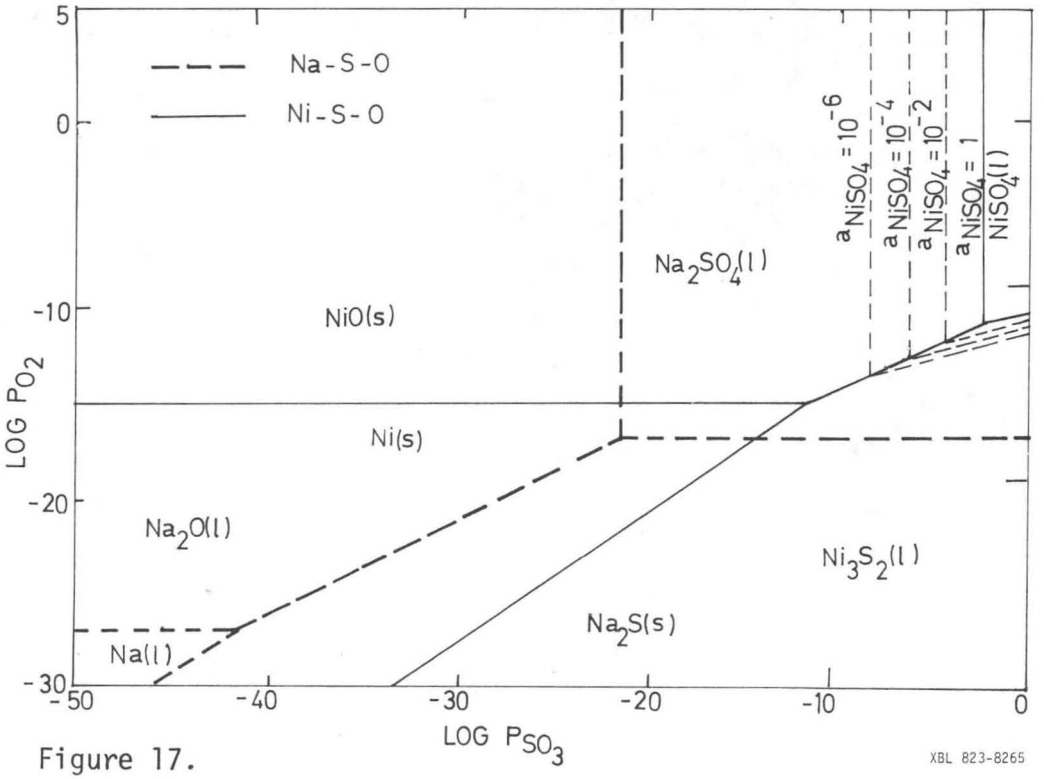
Na-S-O
Ni-S-O
NiO(s)
Ni(s)
Na2O(l)
Na(l)
Na2SO4(l)
Na2S(s)
Ni3S2(l)
aNiSO4 = 10^-6
aNiSO4 = 10^-4
aNiSO4 = 10^-2
aNiSO4 = 1
NiSO4(l)
LOG PO2
LOG PSO3
5
0
-10
-20
-30
-50
-40
-30
-20
-10
0
XBL 823-8265

Figure 17.

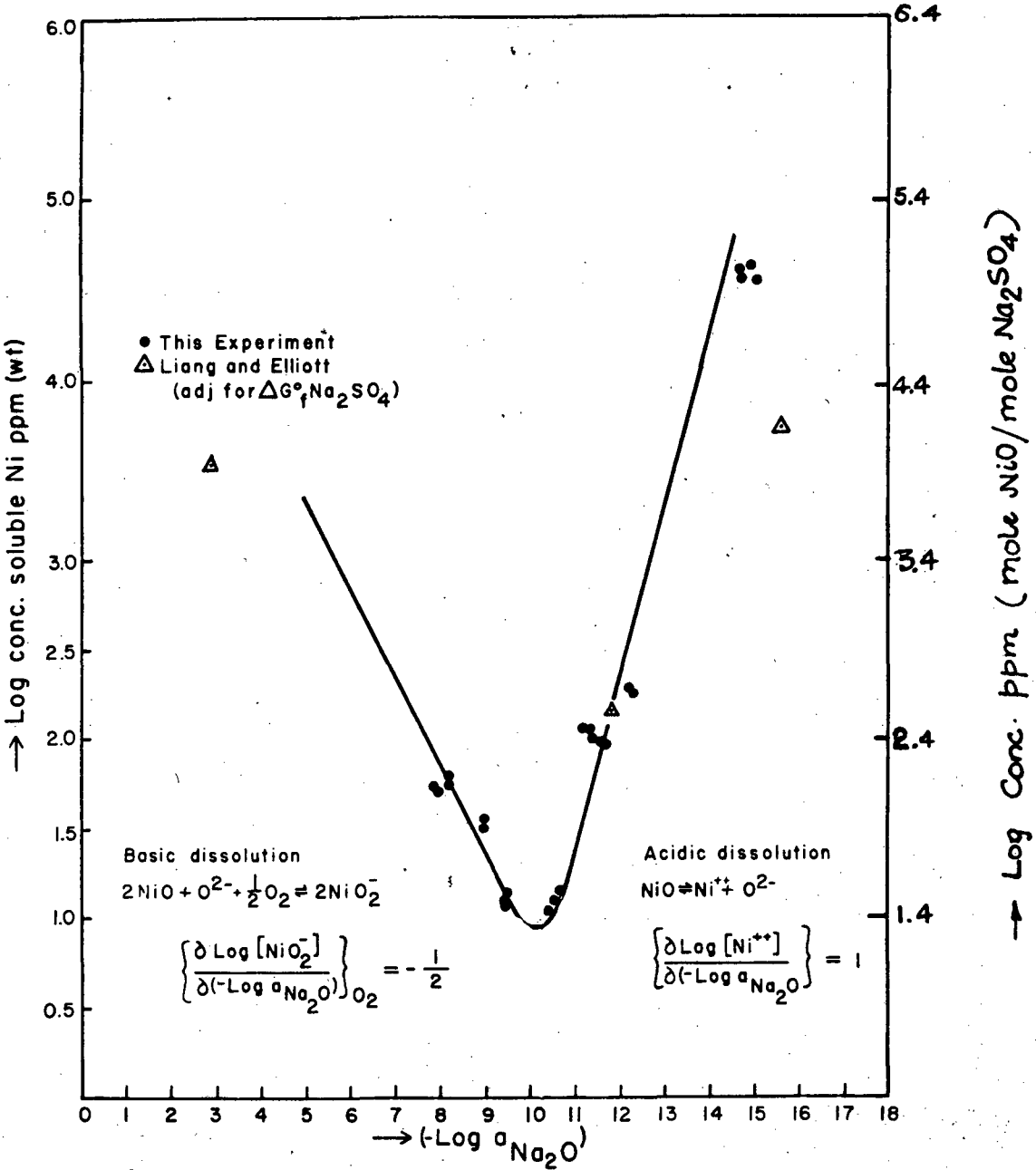

Figure 18.

XBL 809-11576

TECHNICAL INFORMATION DEPARTMENT
LAWRENCE BERKELEY LABORATORY
UNIVERSITY OF CALIFORNIA
BERKELEY, CALIFORNIA 94720